Calcium Carbonate Formation by Genetically Engineered Inorganic Binding Peptides

Carolyn Gayle Gresswell

A thesis

submitted in partial fulfillment of the

requirements for the degree of

Master of Science

University of Washington

2012

Committee:

Mehmet Sarikaya

Candan Tamerler

Daniel Ratner

Program Authorized to Offer Degree:

Department of Materials Science and Engineering

University of Washington

Abstract

Calcium Carbonate Formation by Genetically Engineered Inorganic Binding Peptides

Carolyn Gayle Gresswell

Chair of the Supervisory Committee:

Professor Mehmet Sarikaya

Materials Science and Engineering

Understanding how organisms are capable of forming (synthesize, crystallize, and organize) solid minerals into complex architectures has been a fundamental question of biomimetic materials chemistry and biomineralization for decades. This study utilizes short peptides selected using a cell surface display library for the specific polymorphs of calcium carbonate, i.e., aragonite and calcite, to identify two sets of sequences which can then be used to examine their effects in the formation, crystal structure, morphology of the $CaCO_3$ minerals. A procedure of counter selection, along with fluorescence microscopy (FM)characterization, was adapted to insure that the sequences on the cells were specific to their respective substrate, i.e., aragonite or calcite. From the resulting two sets of sequences selected, five distinct strong binders were identified with a variety of biochemical characteristics and synthesized for further study. Protein derived peptides, using the known sequences of the proteins that are associated with calcite or aragonite, were also designed using a bioinformatics-based similarity analysis of the two sets of binders. In particular, an aragonite binding protein segment, AP7, a protein found in nacre, was chosen for this design and the resulting effects of the designed peptides and the AP7 were examined. Specifically, the binding affinities of the selected and the protein derived peptides off the cells were then tested using FM; these studies resulted in different binding characteristics of the synthesized and cellular bound peptides . Two of the peptides that displayed strong binding on the cells bound to neither of the $CaCO_3$ substrates and both the high and low similarity

protein-derived peptides bound to both polymorphs. However, two of the peptides were found to only bind to their respective polymorph showing; these results are significant in that with this study it is demonstrated that the designed peptides based on experimental library-based selection and sequence identification, can be designed to have recognition capability to a given crystal structure, specifically, in this case, of calcium carbonate. Calcite mineralization with the peptides produced vaterite when several of the peptides were used in the synthesis process, many having unique morphologies studied using scanning electron microscopy (SEM). The amount of vaterite crystal percentage in these biomineralized mixtures was calculated and it was found to be closely related to peptide concentration for the aragonite-binding peptides. In the aragonite mineralization experiments, a separate solid phase, namely, calcium nitrate hydrate, was produced for one of the peptides along with the other polymorphs of calcite carbonate (ie., aragonite, calcite and vaterite) in the solution in the form of a flat film. These biomineralization results are examined in the light of the effects of peptide sequences and their related solid-binding characteristics

TABLE OF CONTENTS

LIST OF FIGURES

LIST OF TABLES

ACKNOWLEDGEMENTS

I am grateful to all those that helped me with this project and made it a success. I owe my deepest gratitude to Professor Mehmet Sarikaya for providing guidance and the mentorship that has altered the way I approach scientific problems. I would also like to thank Professor Candan Tamerler for her help and her incites to the biological aspect of my projects.

It is my pleasure to thanks those that made this thesis possible, my examination committee: professors Mehmet Sarikaya, Candan Tamerler and Daniel Ratner. Thank you again for evaluating my work.

I am also grateful for assistance received from Dr. Marketa Hnilova, for teaching me cell surface display and giving me assistance and guidance. I would also like to thank Dr. Ersin Emre Oren, for undertaking the similarity analysis and Dr. Hanson Fong for teaching me the SEM and TEM. . Finally I would like to express my appreciation to my fellow grad students, Chris So, Dmitriy Khatayevich, Tamon Page and Mustafa Gungormus; I appreciated all their advice and guidance that they have given me over the years as both coworkers and as friends.

Chapter 1: Introduction

For millions of years, Nature has created complex mineral systems that have unique mechanical properties due to their delicate organization of inorganic materials that have been molded into intricate architectures. The most well known and abundant of these biominerals is calcium carbonate ($CaCO_3$).[1] Calcium carbonate is found in diverse geography and geology all over the world. Technologically, its one form or another has been used in almost every industry from paper (as filler particles) to pharmaceuticals. Even though humans have been using this mineral for hundreds of years, the current technology is nowhere close to the level of control that Nature exhibits over this material's formation, crystallography and morphology. Many researchers over the last 100 years have studied to learn and gain lessons from the ways Nature has been able to create these complex composite materials in a variety of forms using just the specialized proteins as their tools.[2, 3] In spite of these extensive studies, however, the exact mechanism(s) of calcium carbonate (for that matter any kind of) biomineralization are still not very well understood. Calcium carbonate is also used as a model system for understanding polymorph determination in biology, which can then be utilized for different practical applications in everyday technology. Mainly because of the complexity of the naturally occurring proteins and their multi-faceted effects on variety of biofabrication, the study of biomineralization using these have been next to impossible so far.[4] This study, therefore, was designed to explore, the effect of combinatorial selected short polypeptides on biominealization in a molecular biomimetics platform. Specifically, using a cell-surface display library, two sets (containing more than 50 sequences each) of dodecapeptides were selected using two forms of $CaCO_3$, aragonite and calcite, as substrates; these peptides were characterized in terms of their binding characteristics to the respective forms of carbonates and then mineralization assays were generated using several of the peptides from each set to find out if they are able to exhibit specificity in binding and a control over polymorph formation through well-established biomineralization assays.

1.1. Polymorphs of Calcium Carbonate and Their Normal Existing Conditions

In order to understand calcium carbonates' versatility in biology and industry, one must first recognize the different crystal structures that it possesses. Calcium carbonate exists in three anhydrous crystalline forms: calcite (R), aragonite (O) and vaterite (H) and two hydrated forms: calcium carbonate hexahydrate and calcium carbonate monohydrate.[1, 5, 6] There is also an

amorphous form which is highly unstable at standard conditions.[1] The anhydrous structures are the most commonly found although some are more prevalent than others.

Calcite is the most abundant polymorph since it is thermodynamically stable under ambient conditions of room temperature and atmospheric pressure, and has a Gibbs free energy of -1129.176 kJ/mol.[7] This low ΔG originates from the fact that calcite has a face-centered rhombohedral unit cell that allows for the distance between the calcium atom and the oxygen atoms to be shorter than any other crystal structures of $CaCO_3$, as seen in figure 1 (a).[1, 5] Even though the distances between these atoms are very small, the overall density of the calcite mineral is actually quite low compared to, for example, the aragonite phase. The density of calcite is 2.71 g/cc while that of aragonite is 2.93 g/cc; this difference is due to the unique packing of the aragonite structure that allows the CO_3^{-2} ion groups to be closer to Ca^{+2} ions than those in calcite.[5] The aragonite phase (orthorhombic) has a slightly more positive gibbs free energy of -1128.355 kJ/mol compared to calcite. [7] Even though aragonite is metastable, if stored in dry conditions it will remain unaltered for tens of millions of years at temperatures below 400°C.[5] If water is present, however, aragonite will convert to calcite in a matter of months due to its greater solubility in water.[5] The difference in solubility is one of the reasons why aragonite is not as common in geological beds and is rarely found outside of organically controlled systems. As seen in figure 1 (b) the calcium ion is very close to the limiting value for transition making aragonite's orthorhomobic structure fairly easy to shift into the thermodynamically stable rhombohedral structure, though depending on approach the activation energy ranges from 159 to 452 kJ/mol.[1, 5, 6]

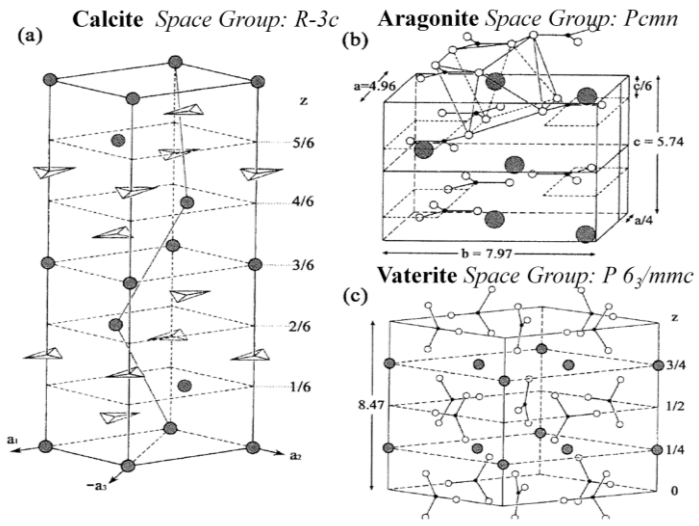

Figure 1: Unit cells of the three anhydrous CaCO3 polymorphs: a) calcite b) aragonite c) vaterite1 Grey circles are calcium, white circles or line endpoints are oxygen and black dots are carbon.

The kinetically favored polymorph of calcium carbonate is vaterite, which has a hexagonal unit cell with the CO3 groups parallel to the c-axis (fig 1 (c)).[1] This metastable form has a density of 2.65 and requires a loosely packed structure which coincides with its low stability.[5] Vaterite is rarely found in nature since it is not thermodynamically favored and will often transform quickly into one of the other anhydrous polymorphs. If inhibitors to the calcite and aragonite polymorph are present however, vaterite can stabilized, which is why it is commonly found in laboratory experiments.

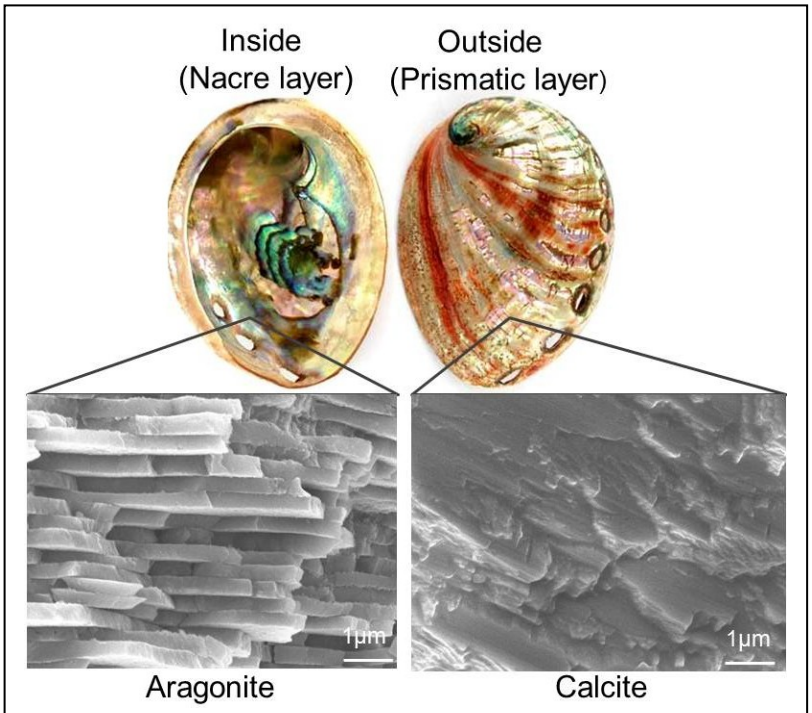

Figure 2: Abalone shell image with a SEM image of the nacre and prismatic layer at 15,000X magnification

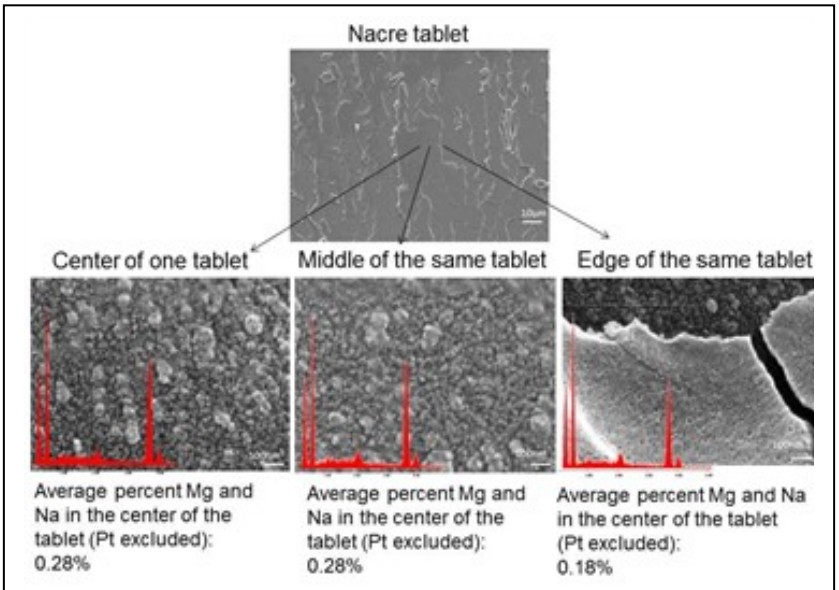

Figure 3: SEM and EDS showing the average magnesium percentage for different areas of a nacre tablet within an abalone shell.

1.2. Calcium Carbonate in Nature

Throughout nature organisms have created structures out of inorganic minerals, with up to 60 biominerals being recognized, but none have achieved the prevalence of $CaCO_3$ within biological systems.[1] This extensiveness has led to a wide variety of functions and unique architectures. Different arrangements of $CaCO_3$ have been known to increase its strength from 30MPa in its geological form to between 100-300MPa in shells.[8] Mollusks that live in colder environments, fresh water or have high levels of predation tend to form the toughest shells

that have two different polymorph layers. The top prismatic layer (calcite) and the inside, nacre layer, (aragonite) helps protect the mollusk within by exemplifying the different physical properties of these crystal structures as seen in figure 2. In environments lacking high Mg concentration calcite is necessary on the outside of the shell to slow the dissolution of the ions back into the environment. Even though it does not have a well-defined microstructure the prismatic layer also has a higher compressive strength than the inside and acts like armor protecting the creature from piercing damage.[9] The nacre layer on the other hand is arranged in a brick and mortar configuration where aragonite tablets are stacked with an organic layer in between. This formation prevents uncontrolled crack growth if the stress is normal to the shell while if it is shear stress the tablets are able to slide over each other with the help of the organic matrix.[9] Also this inside layer has a very high bend and tensile strength that further deters predators.[9] Along with this being in two different crystal structure layers produces residual stresses that help absorb energy from the impact further lengthening the time before failure.[10]

Another unique finding of these shells is the lack of Mg that is incorporated within these layers even though the surrounding fluids contain a significant amount of this ion. Mollusk's extrapallial fluid where they build the shells has a similar ratio of magnesium to calcium as the surrounding ocean which can vary from 3:1 to 5.2:1 depending on the location.[11],[12, 13] In one of Gower's papers she shows that with a 3:1 and 5:1 ratio of Mg to Ca and same amount of polymer added there is 20% to 30% of Mg incorporating into the films.[14] From the EDS on three different locations on several nacre tablets of an abalone shell there is an average of less than one percent on any particular area as seen in figure 3. These results are consistent with those in the literature which is around 60ppm of Mg in aragonite shell layers.[15] The level of control of all these aspects is done by the organism's use of proteins to organize this amazing biomineral.

1.3. Calcium Carbonate in Industry

Calcium carbonate is found in almost every major industry due to its versatile nature. In ancient societies shells were used as prestige goods that were fashioned into jewelry or other ornaments.[16] Today shells and pearls are still prevalent in the jewelry industry for their unique appearance. In pharmaceuticals $CaCO_3$ is found in calcium supplements as well as is often the binder in many chewable pills.[17, 18] The paper and paint industry use $CaCO_3$ as a filler or pigment due to its high brightness and apparent light scattering coefficient.[19] In the paper industry the size of the filler particles are very important since it determines how stiff and glossy the page

is.[19] In the construction industry $CaCO_3$ is found almost everywhere since it is a major component of marble and limestone which is used in cement. Nature long ago realized $CaCO_3$'s building potential and has been using proteins to model with it for millions of years.

1.4. Proteins Effect on Calcium Carbonate Formation

Proteins are known to be the main component that controls $CaCO_3$ polymorph and morphology in organisms. In vitro studies of the protein mixture from mollusk nacre layer shows that they are able to reproduce the polymorph and morphology of the natural material just given the basic components found in the extrapallial solution.[20] Chitin, a major structural component of shellfish, was also present in this experiment, which may have an influence on the formation mechanisms. Beta-Chitin in particular has been used as a template for many experiments since it was found in the nacre layer of certain mollusk shells, though how this molecule is used by the organism is not very well understood.[21] In order to discover which proteins were responsible for polymorph control, other researchers have separated several from this nacre mixture and tried them individually in vitro. Different species of shellfish that are known to construct with $CaCO_3$ were also used to gather more proteins that may influence crystal structure. So far there are 16 proteins that are known to associate with $CaCO_3$, from six different species of mollusk and one from fish otolith, composed of aragonite and vaterite.[22-36] Perlucin and Perlustrin were the first two proteins that had been separated from the chitin layer of *Haliotis Laevigata* and showed that perlucin may nucleate calcium carbonate quicker than the control.[31] From the japanese pearl oyster (*Picntada fucata*) six proteins were extracted from different areas and called: N16, ACCBP, Nacrein, CaLP, n19, PFMG1, Aspein and Prismalin14.[24, 29, 30, 32, 34, 36] N16 has been shown to form aragonite in certain cases but it needs the help of beta chitin a structural matrix found within certain marine animals generally squid.[27, 37] PFMG1 is also able to create aragonite, in nanoparticle form though with TEM it is uncertain how prevalent this polymorph is in the solution.[29] ACCBP creates rounded calcite crystals while nacrein has an inhibitory effect on crystal formation and maybe involved in regulating the size of aragonite crystals in vivo.[32, 38] Aspein and Prismalin14 are both extracted from the prismatic layer and while the former promoted $CaCO_3$ formation the latter inhibited it.[35, 36] Five proteins called: AP7, AP24, AP8α, AP8β and Lustrin A, were separated from the pacific red abalone (*Haliotis rufescens*) while only Asprich originates from *Atrina rigida*.[23, 26, 28, 33] Calprismin is from the species *Picntada nobilis* and controls $CaCO_3$ shape while MPSP is from *C. gigas* and is a promoter.[34] AP7 creates

irregular step edges when mineralized with Kevlar threads, but without this ionic substrate this protein is able to create aragonite.[33, 39] AP24 causes interruptions in crystal growth and step edges on calcite while AP8s rounds these crystals in on Kevlar thread.[23, 25] Asprich creates twinning in calcite crystals.[40]

Some researchers also use fish otolith to find proteins that bind to $CaCO_3$ and affect growth.[22] Unfortunately many of the protein are very difficult to separate from one another in the otolith so for many of their experiments the researchers had a mixture of high molecular weight proteins which has been shown to form aragonite when attached to sepharose beads. These same researchers were able to separate out one protein they called otolith matrix macromolecule-64 which produced vaterite when attached on a sepharose bead.[22]

From the sequences of these proteins certain trends were found in amino acid composition and conformation. In all these proteins there is normally presence of interactive sequence clusters with either hydrogen bonders or acidic amino acids.[33, 41] All proteins with known structures have an unfolded conformation, which may permit adaption with exposed material or promotes ion clustering.[42, 43],[34] Also having planar surfaces on polypeptides appears to play an important role in nucleation and surface interactions.[34]

1.5. Polymer Effect on Calcium Carbonate Mineralization

Polymers have been used for many years to control the morphology and polymorph of $CaCO_3$. Though these exact molecules have never been found in nature they are used to give researchers a better idea of potential mechanisms for $CaCO_3$ formation. One of the many discoveries found using polymers was that there was a polymer-induced liquid-precursor (PILP) process.[44] This process allows films to be made from stabilized amorphous calcium carbonate, which will eventually transform into calcite over time.[45] Unusual morphologies can be formed from the PILP process such as layered calcite films which can then create hybrid multilayers and transition bar style coatings of $CaCO_3$.[45-47] Certain polymers are also able to stabilize vaterite in high enough concentrations. Many of the PEG linked block copolymers are believed to form vaterite easily since they have a disordered structure that tends to optimize the number of binding sites to $CaCO_3$.[48] Coelfen et al. was able to demonstrate polymorph control by varying the concentration of $CaCl_2$and the amount of polymer, PSS-co-PNIPAAM in solution.[49] Figure 4 shows a diagram of morphologies based on Ca concentration and polymer concentration along with SEM images of characteristic looking polymorphs formed by different polymer

concentrations.[50-52] From these results they were able to show that the switching between calcite and vaterite can be obtained when there is a strong crystallization inhibiting additive and fast nucleation along with a way to stabilize the vaterite.[49] Heterogeneous aragonite formation was obtained using low concentrations of amorphous nanoparticles and a polar surface with a phyisorbed polymer.[49] Polymers are also able to create very unique calcite structures by inhibiting certain planes of growth.[49, 52] Large molecules are definitely able to affect $CaCO_3$ growth, but small peptides are also able to replicate many of the same morphologies.

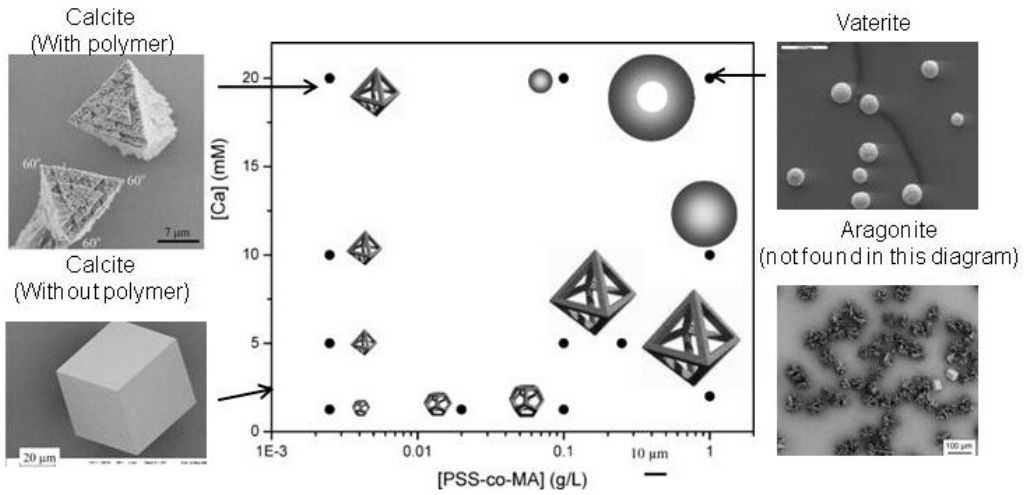

Figure 4. By altering the concentration of PSS-co-MA and Ca^{2+}, Coelfen et al was able to form different morphologies and polymorphs of $CaCO_3$ as seen in the diagram. SEM images are of all the polymorphs that were able to be formed using polymers not just those included in the graph.[50-52]

1.6. Peptide Effect on Calcium Carbonate Mineralization

Peptides are small amino acid sequences that are much easier to synthesize than proteins via conventional methods. For this reason many researchers have also synthesized peptides based off of the protein sequences found from nature. The most common sequences are either the N or C terminus of the protein which encompasses approximately 30 amino acids off one of these ends. Many of these shorter peptides are able to recreate the morphology and results of the whole protein, while being much easier to determine structure and understand the mechanisms of how they work. For example, AP7-N term which is the N-terminus of AP7 also creates irregular step

edges when mineralized on Kevlar, but does not form aragonite, indicating that the remaining part of the protein could be responsible for the switching.[39, 53] The C-terminus of this protein did not show any change from the control so it is unlikely that it is just a sequence issue, but perhaps it is how the two parts of the protein interact to be able to form aragonite.[25] On the other hand the N-terminus of N16 is able to synthesize aragonite, when beta-chitin is added with similar morphology to the complete protein which indicates that this sequence is involved with polymorph switching.[37] AP24's terminus peptides did not show as strong of inhibiting affects as the full length, but were still able to etch the calcite slightly on the Kevlar threads.[54] PFMG1-N term is able form aragonite particles while the C-term is only able to create twinning calcite.[29] D4 is a peptide created from Lustrin A that exhibits calcium and mineralization interactions by changing the morphology of the overgrowth layer.[41]

Computer models have also been used to create peptides that interact with $CaCO_3$. These models normally use charge interactions and other binding motifs to create de novo designed peptides that interact with the $CaCO_3$ surface.[55, 56] These peptides often inhibit growth formation in certain directions since they bind to that area and slow precipitation creating irregular step edges or etching, but so far none have been able to control the crystal structure. [55, 56]

Phage display has also been used to find peptides that bind to $CaCO_3$. One set of researcher just used the phage with the peptide expressed on both calcite and aragonite to see how it would modify $CaCO_3$ growth.[57] They found that their peptides while on the phage would just inhibit the growth of $CaCO_3$ and create some irregularities, but not throughout the entire sample.[57] Another researcher then selected for just calcite and pick a few from the binders and synthesized them.[58] They had slightly better success in the fact that one of their binders stabilized vaterite in their solution, though they did not quantify how much vaterite was present, nor did they give any other selection results.[58] Aragonite has also been used as a substrate for selection and three binders have been selected from this and used in a vapor diffusion and kinetics experiment.[59] In the vapor diffusion experiment the peptides did slight etching to the calcite crystals but in the kinetics they were shown to slow the transformation of vaterite slightly.[59] None of these peptides were classified as strong or weak binders so it is uncertain if binding strength has an effect on being able to control crystal structure. So far no researchers have used cell surface display to find peptides involved with $CaCO_3$ formation, which gives you a different ratio of amino acids present.

Chapter 2: Experimental Approaches

2.1. Selection and Characterization of Peptides (CalBPs and AraBPs) Using Cell Surface Display

Calcite and aragonite binding peptides were selected from the FliTrx random peptide display library (Invitrogen, USA). This library contains FLITRX bacteria that have randomized dodecapeptides inserted into their flagellin protein allowing the bacteria to stick to a specific substrate. The two different polymorphs of calcium carbonate were both from Agate Design in Seattle and considered very pure. Cleavage of calcite was done with a razor while a saw was able to cut the aragonite into approximately 0.5 cm square samples for the panning experiment. Several of these substrates were then cleaned using standard washing procedures where methonal/acetone (50:50), then isoproponal and then deionized water were added to the sample and sonicated after each addition.[60] Three rounds of panning were preformed according to the method developed by Invitrogen on both materials. Afterwards a "counter selection" was done to insure the chosen peptides were specific to a particular polymorph of calcium carbonate. A schematic of the normal and counter selection rounds is shown in Figure 5. For the counter selection the amplified cells from the previous round were incubated with a different polymorph of $CaCO_3$ for 1 hr. Then the substrate was removed and the cells that did not bind were amplified in IMC overnight. Sequencing was done by the University of Washington Microbiology department. Molecular weight, pI and charge were calculated using the ProtParam Tool at expassy.org.

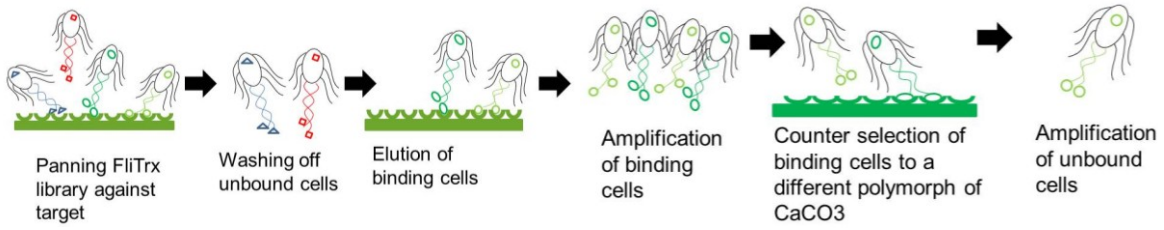

Figure 5: Schematic of cell surface display with counter selection.

FM was used for the characterization experiments of all 86 clones. For the FM characterization, the aragonite was polished to create a more uniform surface while the calcite was freshly cleaved. Binding affinity for the clones was determined by comparing the number of adhering

cells in at least three different fields on the substrate. By comparing the number of cells found on each substrate the clones were sorted into three groups: strong, medium and weak binders.

2.2. Synthesis and Purification of Calcite and Aragonite Binding Peptides (CalBPs and AraBPs)

Calcite and aragonite binding peptides were synthesized using a Fmoc solid-phase peptide synthesizer (CS336X, CSBio Inc., Menlo Park, CA) and purified using C-18 reversed-phase high- performance liquid chromatography (RP-HPLC) to a purity > 95% (Bio-Peptide Co.). During purification, several fractions were collected from the scaled semipreparative separation (Waters Deltaprep 600, semiprep mode). The collected high-peak solutions were later identified by MALDI-TOF mass spectrometry. The purified aqueous peptide was lyophilized overnight in a Vertis Benchtop K cryodessicator (SP Industries, Inc., Warminster, PA).

2.3. Amino Acid Composition Calculations

An expected and observed frequency of occurrence was found for each amino acid based on calculations done by Hnilova et al.[60] To get the expected frequency randomized dodecapeptide were synthesized as (XNN)12, where N was any nucleotide and X was a nucleotide that had a biased ratio of G:A:C:T of 7:7:7:3. The observed frequency was generated by sequencing all 86 clones that bound to substrates and counting the number of each amino acid using protparam. These were then compared to create the relative abundance for a particular amino acid in the set of binders as seen in figure 7.

2.4. Similarity Analysis and Protein Derived Peptides

Protein derived peptides were selected using a knowledge based design approach developed by E. Emre Oren[60, 61]. The binding characteristics of a set of calcite and aragonite binders (CalBP and AraBP) were compared with sequences of naturally occurring proteins to create new peptides with enhanced binding affinities. A similarity analysis was used to make these comparisons that utilized the Needleman-Wunsch dynamic programming algorithm, giving an optimal scoring alignment with a given scoring matrix.[61] This matrix was used to find the overall similarity score by summing all of the similarity values of the aligned residue pairs and subtracting a gap penalty of every insertion or deletion introduced into the alignment.[61] The similarity matrix was then applied to sequences found in nature to determine areas that may function as binding sites.

2.5. Characterization of Synthesized Peptides using FM

Synthesized peptides were functionalized with biotin while still on the resin and purified using RP-HPLC. Calcite and aragonite substrates were first crushed into a fine powder using a mortar and pestle and 10mg of each were weighed out into microcentrifuge tubes and cleaned using the method described in section 2.1. The clean substrates were then incubated with 100µl of 1mg/ml pure peptide stock solution for 2hrs. After this time the substrates were washed with 1X PBS solution twice. Then 50µl of 1:200 diluted fluorescent quantum-dot nanocrystals (QD) were added and allowed to incubate for 15mins. The substrates were then washed 3 times with PBS solution and dissolved in 30µl of this buffer. Only 10µl of this mixture was then plated onto a glass slide and mounted on a Nikon Eclipse TE-2000U Florescence Microscope (Nikon, Japan). This microscope is coupled with a Hamamatsu ORCA-ER cooled charged coupled device (CCD) camera for taking images and a QD605 (exciter 320-460, dichroic 475, emitter 605/40nm Chroma Technology Co, Rockingham, USA) filter set was used for QD detection. The images were recorded through Metamorph Software (Universal Imageing, USA) and the threshold and intensity were normalized to the control which did not contain any peptide.

2.6. Mineralization approach to create calcite without peptides

Calcite was consistently created using a slight modification of the approach developed by Coelfen et al.[62] This method uses vapor diffusion from ammonium carbonate to slowly add carbonate to a $CaCl_2$ system as shown in Fig 6. Instead of using glass beakers for holding the mineralization solution, 10ml petri dishes were used that contained a glass cover slide on the bottom so XRD sampling would be consistent. These slides were cleaned using the same procedure as the substrates in section 2.1 and dried using nitrogen gas. The ammonium carbonate (Sigma) and $CaCl_2$ 97% pure (Riedel-deHaen) were used without further purification. The aqueous solution of $CaCl_2$ (20mM) was freshly prepared before every experiment and 10ml was transferred into the petri dishes. The dishes were covered with Parafilm and several holes were punched into the film to allow for slower diffusion. This was then put into a desiccator with 20mg of the ammonium carbonate in a large petri dish covered with Parafilm punched with several holes. After 24 hours incubating at room temperature (~22 C) in a dark closet the precipitate was removed from the desiccator and rinsed with distilled water and allowed to dry at

room temperature.

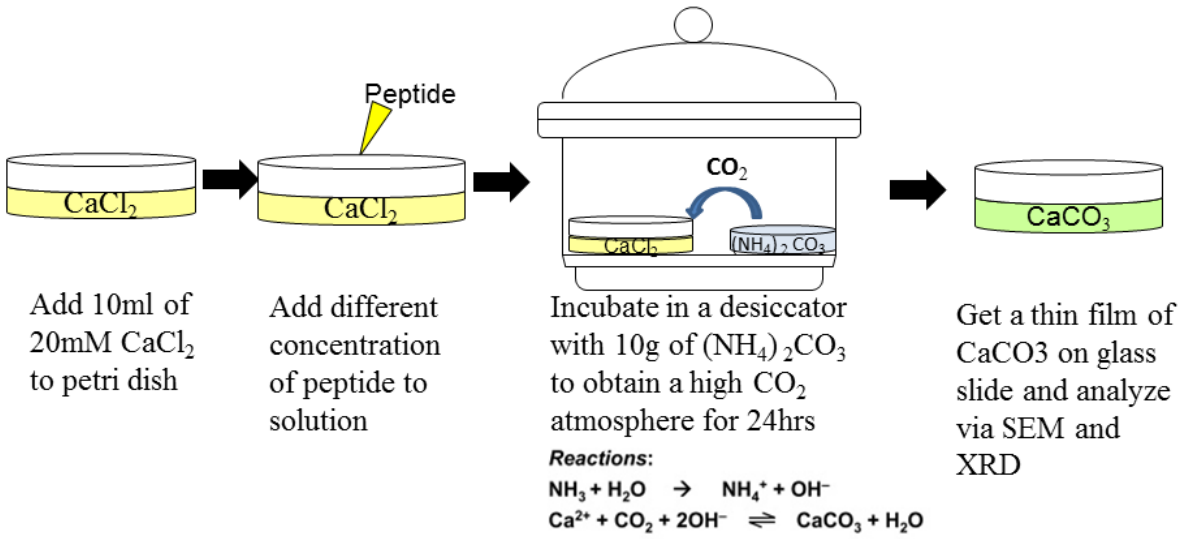

Figure 6: Schematic of biomineralization approach for forming calcite consistently.

2.7. Mineralization approach to create aragonite without peptides

Aragonite was created after optimization of the desiccator method used for creating calcite and magnesium addition using the ratio developed for room temperature aragonite formation by Morse et al.[12] After several optimization steps where the time, the concentration of Mg and the amount of ammonium carbonate were varied separately, aragonite was able to be created though it was mixed with calcite and sometimes vaterite. The precipitate was at least 25% aragonite consistently using the following method. The desiccator method described in the previous section was used with a slight modification. The first modification was adding enough $MgCl_2$ to the $CaCl_2$ solution to get a final concentration of 60mM. Then the amount of ammonium carbonate was reduced to 10mg instead of 20mg in the beginning.

2.8. Mineralization approaches with peptides

Peptides were added to both mineralization approaches to observe formation differences. Amount of peptide was varied to find an optimum level that stabilized the most uncommon polymorph. For the selected peptides three concentrations were tried and for the protein derived peptides only one concentration was tried. Two concentrations (0.05mM and 0.1mM) showed creation of a different polymorph in calcite forming mineralization experiments as well as in

aragonite formation experiments. One other concentration (5mM) was used but did not have enough crystals for either peptide to be able to get an XRD. The peptide was added at the same time as the $CaCl_2$ to the petri dish and mixed by pipetting three times to create an even concentration of peptide.

2.9. Scanning Electron Microscope (SEM)

A JSM 7000F (JEOL) SEM was used at 10kV in secondary electron imaging mode to view particles and discover morphology changes. The $CaCO_3$ samples were first pipetted from the bottom of the petri dish and placed on carbon tape attached to a SEM sample holder. The precipitates were allowed to settle for 10mins and then extra liquid was absorbed using a kimwipe. This was then lypholized for at least an hour before viewing under the microscope.

2.10. X-ray Diffraction (XRD)

Polymorph identification and quantification were performed using X-ray Diffractometer D8 Focus (Bruker) at a constant current of 40mA and voltage of 40 kV. Scans were done in a continuous scan mode at step size 0.02, with time/step = 1 seconds, and a locked coupled angle 2θ between 10 and 95 or 135 degrees. The following slit sizes were used: divergence and antiscatter were set to 0.6 mm, detector was set to 6 mm and monochromator was set to 2 mm. The calcium carbonate samples were allowed to dry over night at room temperature. Slide containing the sample were attached to a polymer holder that allowed x-ray diffraction to occur consistently throughout the entire area. The scans were collected and then analyzed using Jade 7 analytical software, powder diffraction files (PDF) and excel. The percentage of the different polymorphs was calculated using equations from Konotoyannis et al.

Chapter 3: Results

3.1. Sequence Selection

The sequences in Tables 1 and 2 were selected using cell surface display and found using a BDSF's 3730XL sequencer. Strong aragonite binders (AraBP) had an average pI of 8.8 with a standard deviation of 2.9, which was lower than the overall average of 9 +/- 2.5. The strong calcite binders (CalBP) have an average pI around 9.3+/- 2.5 which is higher than the overall 8.5 +/- 3. A general trend for the calcite binders was that the stronger they interacted with the mineral the higher the average pI, while aragonite binders were the opposite. The charge varied considerably from the different binders. For aragonite a charge of zero had the highest prevalence with positive two charges a close second. The charges on the calcite binders varied considerably for the strong binders though most of the strong binders were positively charged.

3.2. Peptide Selection

Peptides were synthesized using Solid Phase Fmoc synthesis described in the experimental section based on their characterization results while still on the cells. Not all the strong binders that showed specificity to a polymorph could be synthesized due to time constraints. For this reason a handful were selected based on the strength of their binding as well as their charge and pI values. Table 3 lists the selected peptides along with their properties that were synthesized for this study.

Amino acid composition among the strong and weak binders of the two different polymorphs was compared to the FliTrx unpanned library to find the relative abundances.

Calculations are found in the materials and methods section. Figure 7 shows that Asp, Lys, and Trp were all overexpressed in all sequences compared to the native library. Also Arg, Asn, Gln, Gly, His, Leu, Met, Pro, Ser, and Val have significant differences in distribution between AraBP and CalBP. The differences between the strong and weak calcite binders were in the Gly, Leu, and Phe amino acids. For the aragonite binders only the Asn amino acid distribution was contradictory.

Table 1: Sequence, molecular weight, pI and charge of aragonite binding peptides

	Clone	Sequence	MW	pI	Charge	Average Cell Count
Strong	4Ara17	GDAACLSLHDMR	1288.4	5.21	-1	61
	3Ara11	VARDPRVRSERG	1397.5	11.52	2	57
	4Ara5	KFAVNWDVGNLI	1375.5	5.84	0	53
	3Ara13	GVEKIVPVSNWA	1298.5	6	0	53
	3Ara9	GGPQCTLMQLLF	1307.5	5.52	0	48
	3Ara5	ARGRAERREQGL	1398.5	11.52	2	41
	3Ara1	QHNLLPLGAVIM	1305.6	6.74	0	40
	3Ara12	QHVREILKGVIR	1447.7	10.84	2	39
	4Ara3	KGEYGLRKPIGW	1403.6	9.7	2	37
	4Ara14	LRRAVHREWTLS	1523.7	11.7	2	36
	4Ara33	QVRRNNLMRHRD	1594.8	12	3	35
Medium	4Ara21	TRGRPCNSDDRD	1391.4	5.84	0	30
	4Ara9	ASRRLAGAELRQ	1327.5	11.7	2	28
	4Ara23	MNVHKRRTRWAQ	1582.8	12.02	4	27
	4Ara2	WGGKVWGDSRGA	1275.3	8.75	1	26
	4Ara22	SSVRLAKRTAVK	1315.5	12.05	4	22
	3Ara17	VTTAHGSDPKAQ	1211.3	6.71	0	20
	4Ara18	RRGSDIKIGDAV	1286.4	8.75	1	19
	4Ara11	TVTPNIQDCKPS	1302.4	5.5	0	18
	3Ara7	AGYRGKSEVIRQ	1363.5	9.99	2	18
	3Ara8	LRREEAGRVIGV	1354.5	9.51	1	17
	4Ara29	HRRRSRTGSPAW	1466.6	12.48	4	16
Weak	3Ara16a	VGVMGVRKVATQ	1244.5	11	2	15
	3Ara10	WASGCRRVRIIA	1387.6	11.7	3	14
	4Ara30	GHGFWGRTRGRH	1423.3	12.3	3	14
	4Ara39	GGRLRLRPRHRW	1559.8	12.6	5	14
	4Ara20	SAEGVTLMRRLV	1331.6	9.31	1	11
	4Ara19	HGFRNSKALTTR	1387.5	12.01	3	11
	3Ara3	QRKIPTHKLQWE	1563.8	9.99	2	10
	3Ara6	GGREAASSAILQ	1159.2	6	0	10
	4Ara16	KWFTHDVGVGGR	1358.5	8.75	1	9
	3Ara4	QVHLGWPVPSIL	1345.6	6.74	0	8
	4Ara8	SLFYSRVVHEHA	1444.6	6.66	0	7
	4Ara36	GGLVVDFSPRPY	1306.4	5.84	0	6
	3Ara2	CSRGGKDGLQCK	1251.4	8.9	2	3

Table 2: Sequence, molecular weight, pI and charge of calcite binding peptides

	Clone	Sequence	MW	pI	Charge	Average Cell Count
Strong	1Cal6	VDKRIGEGGPGR	1240.3	8.72	1	31
	1Cal13	SGTCLLHDSEKA	1260.3	5.3	-1	31
	1Cal15	PLSSRQCRPVNS	1343.5	10.39	2	29
	1Cal17	LSLPHFRSRRIQ	1509.7	12.3	3	28
	4Cal 31	GVSRQSAILHLC	1283.5	8.26	1	23
	2Cal15	STSGRKGFVIPP	1245.4	11	2	21
Medium	2Cal12	RRWDWVLKPVNG	1525.7	10.84	2	16
	2Cal20	GIGGCMGDRVAI	1148.3	5.83	0	16
	4Cal 30	RLRVREWMPLTT	1557.8	11.7	2	16
	1Cal7	RGCEVGSRSIAN	1248.3	8.25	1	16
	2Cal9	QYYQRKRNSHID	1607.7	9.7	2	15
	4Cal 7	GTTCRYLMKGGR	1342.6	10.05	3	13
	3Cal28	KVGGAGGRLLLG	1097.3	11	2	13
	3Cal9	LIGGVAVSANAR	1127.3	9.75	1	11
	3Cal7	RVWLSGGAKGAG	1158.3	11	2	11
	4Cal 23	LAWWMNLQATPG	1387.6	5.52	0	11
	3Cal2	GRKVGLRSVSNT	1273.4	12.01	3	11
	2Cal13	IKGVLVQNAADE	1256.4	4.75	-1	10
	4Cal 13	MVRSWRGSVGLL	1360.6	12	2	10
	3Cal29	RTWLWSHDVVTG	1456.6	6.74	0	10
Weak	3Cal20	VGRSSSRLGRAG	1202.3	12.3	3	9
	2Cal5	TFKGEATFPARG	1281.4	8.41	1	9
	2Cal6	EIFANGGLCMRR	1366.6	8.35	1	8
	3Cal23	VRRRPSRLEGFE	1501.7	11.52	2	8
	4Cal 1	AAPERGPTPIAQ	1207.3	6.05	0	8
	2Cal8	EPAKSASPIVAM	1200.4	6.1	0	8
	1Cal18	RLTWMLVKVVLF	1504.9	11	2	7
	4Cal 28	SGRGRARGPTLI	1240.4	12.3	3	7
	3Cal14	GGWLEDTLIVDL	1330.5	3.49	-3	7
	3Cal19	AGGCAKQESERD	1250.3	4.87	-1	7
	3Cal25	QLAKRKPHKAKG	1361.6	11.33	5	7
	3Cal16	RGLRWTGLIPGV	1324.5	12	2	7
	3Cal24	ELANEFECNIRR	1493.6	4.79	-1	7
	4Cal 11	GKRSASMAQKSS	1237.4	11.17	3	7
	4Cal 17	TGLKPHRIGDEG	1279.4	6.42	0	7
	4Cal 9	AGKKPPRMSGKS	1243.4	11.26	4	7
	1Cal3	GWFSLGTDGTQS	1255.3	3.8	-1	6
	4Cal 15	FTVHIEIPGGSA	1227.3	5.24	-1	6
	4Cal 21	KGAAEADDAGFV	1150.2	4.03	-2	6
	2Cal14	SLRNIKMGSEGM	1322.5	8.46	1	5
	3Cal21	AVRWRGVLRGGA	1297.5	12.3	3	5
	1Cal11	LLIKPKMATLVK	1354.8	10.3	3	4
	2Cal11	EAEYVGLHVLEA	1329.4	4.24	-3	4
	1Cal10	RHRKLKVGVNIR	1475.8	12.31	5	4
	1Cal14	PGRIGIPYRRSP	1368.6	11.71	3	4
	2Cal3	KGSMWRCANLLV	1377.6	9.51	2	3
	4Cal 22	RLAYPGDEEKVL	1389.5	4.68	-1	3
	1Cal20	DTAFVADISVGS	1181.2	3.56	-2	2
	4Cal 12	ACENKRMDIGSE	1352.5	4.94	-1	2
	1Cal1	VAIIPGAFLEKG	1214.4	5.97	0	2
	2Cal19	WKSETIWGQRRM	1577.8	10.84	2	2
	3Cal30	TGVVSGDGKGGT	1034	5.5	0	1

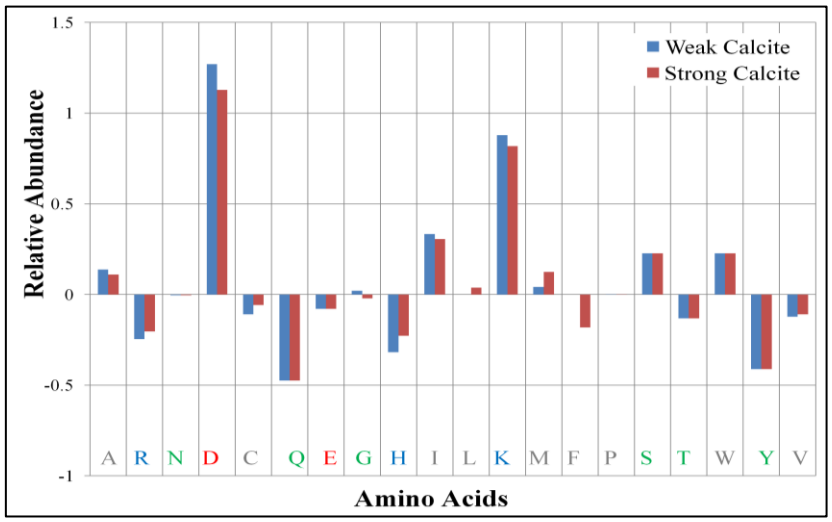

(a)

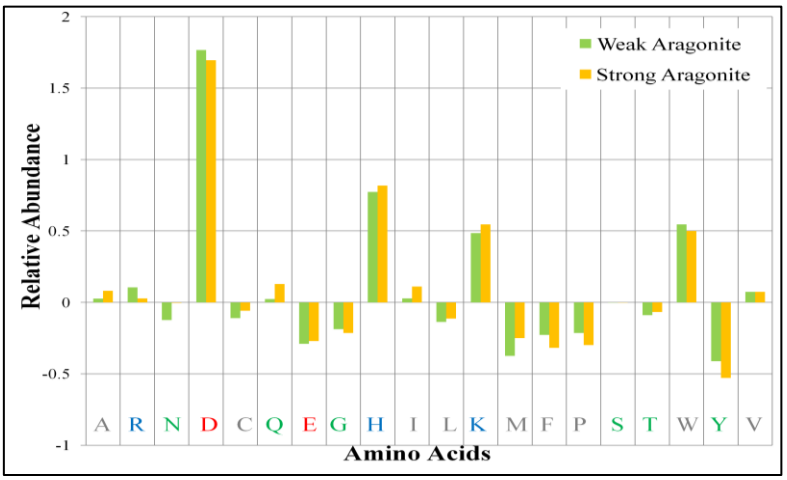

(b)

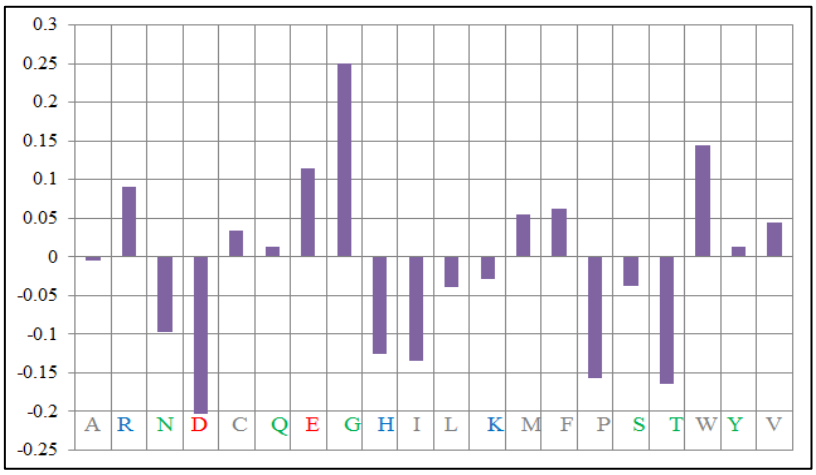

(c)

Figure 7: Relative abundance of amino acids in strong and weak groups of a) calcite and b) aragonite binding peptides and c) cell surface display's observed vs. expected percent differences. The columns are colored as blue = weak calcite, red = strong calcite, green = weak aragonite and yellow = strong aragonite binders. The numbers on the side are percentage away from the observed for the first two graphs and away from the expected for the last graph. The amino acids are colored by hydrophobicity and charge. Grey-Hydrophobic, Green-Polar, Red-Negatively Charged and Blue-Positively Charged

Table 3: Properties of aragonite and calcite binding peptides that were used in this study
Positively Charged AA (K,R) – blue, Negatively Charged AA (E,D) – red, Hydrophobic AA (A,I,L,M,P,V,G) – grey, Polar AA (N,Q,S,T,C) - bright green, Aromatic AA (F,W,Y) - orange, Histidine (H) - light blue, pI and charge computed using ProtParam Tool at expassy.org

Name	Sequence	MW	pI	Total Charge	Polymorph it binds to	Average cell count	Std Dev
3Ara11	VARDDRVRSERG	1415.5	11.52	1	Aragonite	57	5
Charge	0 0 +- - + 0 + 0 - + 0						
4Ara17	GDAACLSLHDMR	1288.4	5.21	-1	Aragonite	61	10
Charge	0 – 0 0 0 0 0 0 – 0 +						
4Ara33	QVRRNNLMRHRD	1594.8	12	3	Aragonite	35	8
Charge	0 0 + + 0 0 0 0 + 0 + -						
1Cal13	SGTCLLHDSEKA	1260.3	5.30	-1	Calcite	31	14
Charge	0 0 0 0 0 0 – 0 -- + 0						
1Cal17	LSLPHFRSRRIQ	1509.7	12.30	3	Calcite	28	3
Charge	0 0 0 0 0 0 + 0 + + 0 0						

1Cal13 was chosen for its high binding affinity to calcite along with its large amount of polar amino acids and negatively charged amino acids which were unusual in the selection. Even though 4Ara17 has a negative charge as well, it also has a large amount of hydrophobic amino acids that may interfere with the charge being displayed in the solution. 1Cal17 was chosen since it has the highest pI of all of the strong binding sequences and contains an aromatic amino acid along with its high binding affinity to calcite. The following sections go into more detail on the peptides characterizations and their effect on $CaCO_3$ mineralization.

3.3. Characterization results

Characterization of the genetically engineered peptides (GEPIS) was done while they were still on the cells and after the strong binders were synthesized in order to find the binding capabilities to the different polymorphs. These methods were used rather than SPR and QCM for characterization because $CaCO_3$ can dissolve in flowing water and create a difference in mass which can alter the binding results.

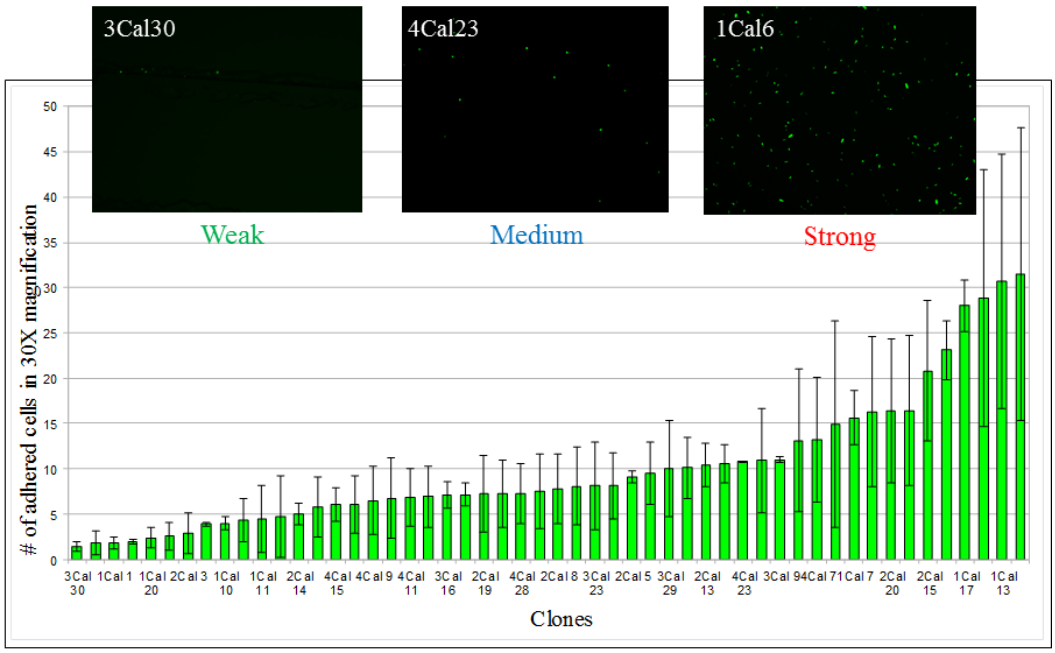

(a)

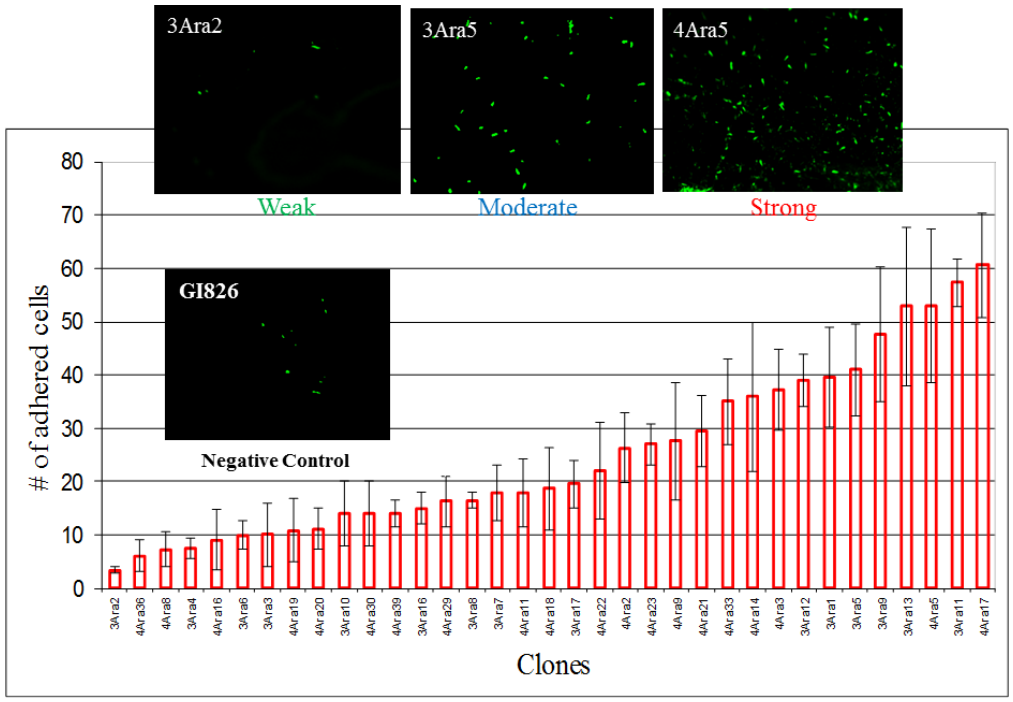

(b)

Figure 8: Characterization of sequences while still incorporated in the flagella of the E. coli: (a) Cell counts of calcite binding peptides on a calcite substrate, magnification 30X. (b) Cell count of aragonite binding peptides on aragonite substrate, magnification 20X (Courtesy of Marketa Hnilova).

3.3.1. Characterization of cells with peptide on flagella

Peptides' binding strength towards a selected substrate was characterized using FM while still on the flagella of the E.Coli. Figure 8 (a) shows the results of this characterization for CalBPs on calcite while Fig 8 (b) shows AraBPs on aragonite. The labeling of the peptides has been changed from those present on the graphs in order to simplify and prevent confusion. Arbitrary cuts off were used to determine which peptides were considered strong, medium and weak binders. The cut off for the calcite binding peptide was anything below 10 adhering cells was considered a weak binder while anything above 20 cells was considered a strong binder and everything in between a medium binder. For the aragonite binding cells a count below 20 cells was a weak binder between that and 40 cells a medium binder and above 40 cells a strong binder. The cutoffs were higher for the aragonite binders because of the larger sampling size due to lower magnification.

For the strong binding peptides further characterization was done to determine if the binding was specific to a polymorph or if the peptide bound indiscriminately to any crystal structure of $CaCO_3$. Figure 9 (a) shows the strong binders for aragonite on calcite and Fig 9 (b) shows calcite CalBP are specific to calcite while only 4 out of the 7 strong AraBP don't bind to calcite. This shows that even when doing a counter selection it is difficult to insure that peptides are specific to only one polymorph of an element.

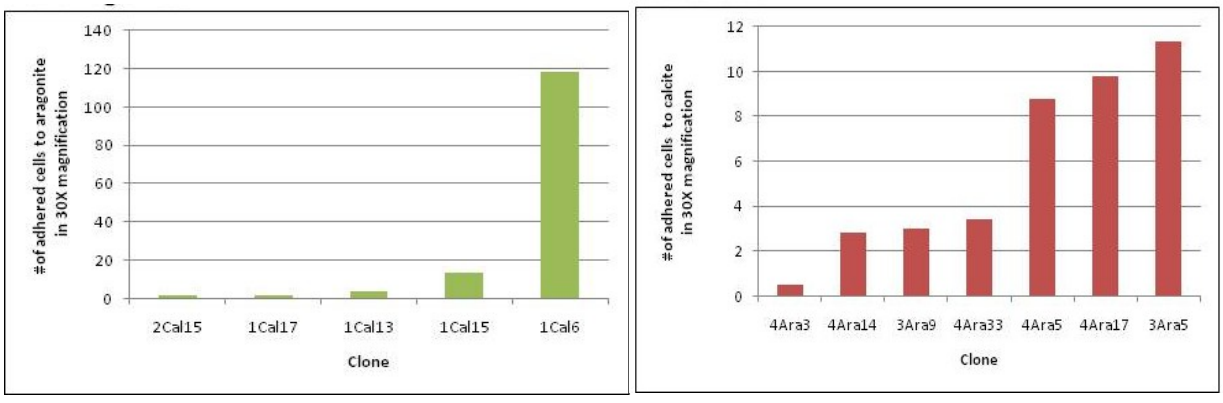

(a) (b)

Figure 9: Specificity of sequences to their specific polymorph while still incorporated in the flagella of the E. coli. (a) Cell count of calcite binding peptides on aragonite substrate. (b) Cell count of aragonite binding peptides on calcite substrate. Magnification 30X.

3.3.2. Similarity Analysis and Protein Derived Peptides

A similarity analysis was done on all of the characterized peptides to determine if the strong binders were more alike than the weak binders. Below in Fig 10 are the analyses of both sets of peptides which show the predicative power of the calcite binding analysis being 64% while for the aragonite binders it is 82%. The predictive power is an estimation of the chance of forecasting if a sequence is going to be a strong or weak binder for that specific substrate. The Needleman-Wunsch dynamic programming algorithm gives the optimal scoring alignment given a scoring matrix. The scoring matrix created by Oren iterative perturbs the known scoring matrices BLOSUM 62 and PAM 250 using a greedy procedure.[61] Both the total similarity scores (TSS) of the strong binders (TSSs-s) and the cross-TSS between strong and weak sequences(TSSw-s) were calculated after every perturbation.[61] Only perturbations that increased the difference between the TSSs-s and the TSSs-w were accepted to create the scoring matrix. The TSS were normalized according to equation 1 shown below:

$$[1] \qquad TSS_{A-B}([A]_{NA} - [B]_{NB}) = \frac{1}{NA \cdot (NB - \delta_{AB})} \sum_{i=1}^{NA} \sum_{j=1}^{NB} PSS_{ij}(1 - \delta_{ij}\delta_{AB})$$

Where, δ is the Kronecker delta function ($\delta_{ij} = 1$ *if* $i = j \wedge \delta_{ij} = 0$ otherwise 0). *NA* and *NB* are the number of sequences in sets *A* and *B*, and PSS_{ij} is the pairwise similarity scores (PSS) value between the i^{th} sequence of set *A* and j^{th} sequence of set *B*.[61] Once the scoring matrix was generated the overall similarity score for a pairwise alignment could be calculated by adding all the similarity values of the residue pairs together minus a gap penalty for insertion or deletions introduced for each sequence. The formula $g(k) = -\text{gop} - (k-1)\text{gep}$ was used to penalize gaps where k is the length and gop and gep are the gap openings and extension penalties.[61]

Using this analysis on a natural protein a peptide was designed and synthesized to see if it would be the aragonite binding domain on that protein. The natural proteins that were considered to have a domain that bind to aragonite were: AP7, AP24, Nacrein, N16, and Lustrin A. Using the similarity analysis developed for aragonite the different areas in the protein sequence were compared with the strong binders found using CSD to see how close they match. This involved calculating the TSS between each of the amino acids and the corresponding area of the protein. Amino acids were given a score based on their similarity to the strong binders as seen in figure 11. Areas that had a very high similarity to the strong binders were recorded as well as those that

had a very low similarity. The red line in figure 11 indicates which amino acids sequences were similar enough to the strong binders to be considered as potential aragonite binding areas. Cut offs for the strong and weak binders were arbitrary, but corresponded with values that were well above or below the average. The red box in figure 11 indicates the sequence that was chosen as a high similarity sections while the blue box indicates the section that has a very low similarity to the strong binders. The structure of the protein was also estimated using HyperChem to see if the sequences would be easily accessed or if they were folded inside the protein. The AP7 protein was the only one that had a sequence with a very high similarity that could also be easily accessed for binding. Table 4 has the high similarity and low similarity sequences found in AP7.

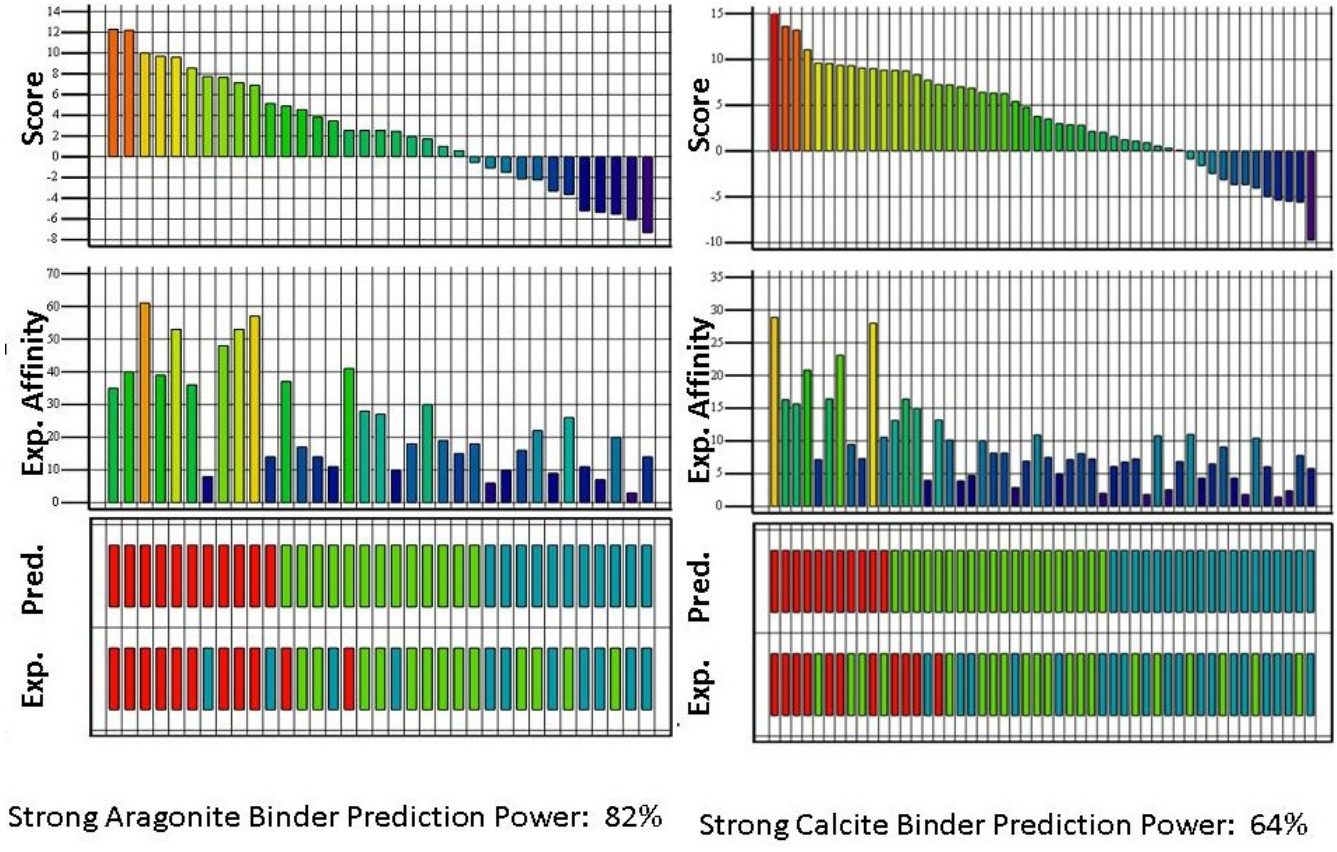

(a) (b)

Figure 10: Similarity analysis of selected peptides (a) Calcite (b) Aragonite

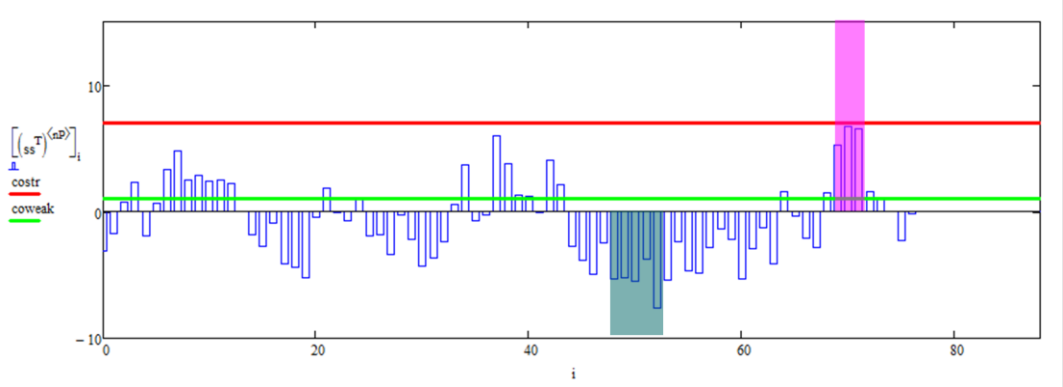

AP7:
MTYMCSILICLVLILCARGAEADDNGNYGNGMASVRTQGNTYDDLASL**ISYLTRHSFRRPFHE**
CALCYS**ITDPGERQRCIDMY**CSYTN

Figure 11: Graphical comparison of AP7 with strong aragonite binders using similarity analysis. The x-axis shows the TSS score while the y-axis is the amino acid number counting from the N-terminus. The amino acids highlighted in blue have low similarity while the pink ones have high similarity.

Table 4: Properties of Protein Derived peptides that were used in this study
Positively Charged AA (K,R) – blue, Negatively Charged AA (E,D) – red, Hydrophobic AA (A,I,L,M,P,V,G) – grey, Polar AA (N,Q,S,T,C) - bright green, Aromatic AA (F,W,Y) - orange, Histidine (H) - light blue, pI and charge computed using ProtParam Tool at expassy.org

Peptide Name	Sequence	pI	Charge	Similarity to aragonite binders
AP7-PDP1	ITDPGERQRCIDMY	4.56	-1	High Similarity
AP7-PDP2	ISYLTRHSFRRPFHE	9.50	2	Low Similarity

3.3.3. Characterization of synthesized peptides

Further characterization was done on the CalBPs, AraBPs and the protein designed peptides after being synthesized. These experiments were preformed in order to find the binding strength of the actual peptide without interference from the cell which may have affected the binding since they are much larger than the peptide. A schematic of the approach is shown in Figure 12. Also this experiment allows for better quantification of the binding for the actual peptides using the threshold calculator on the Metamorph software. The images in Figure 13 were normalized with respect to the control, which was incubated with Qdots but was not incubated with peptide. The normalization is necessary because Qdots can sometimes bind to a substrate even if no biotinylated peptides are present. From the images is it very hard to tell the two different protein designed peptides apart since they both bind well to aragonite and slightly less to calcite which is

why threshold calculations were used. Along with this 4Ara17 was not able to be biotinylated effectively and so was not able to be characterized in this fashion.

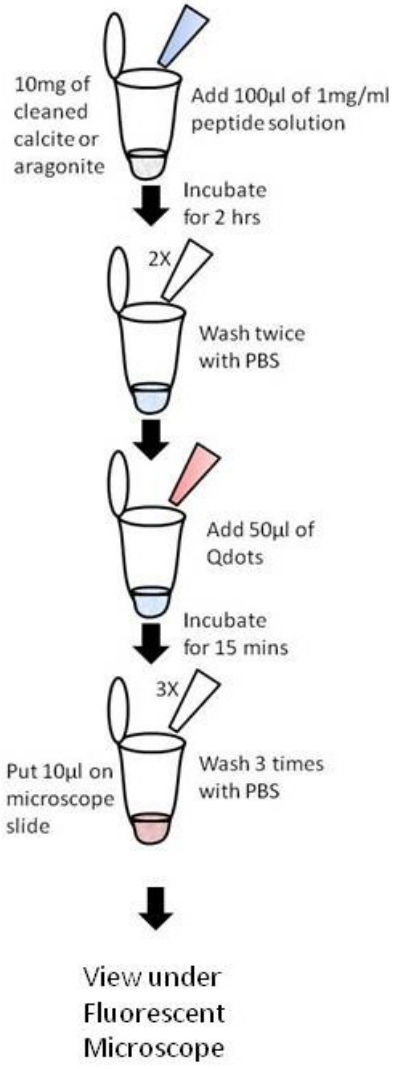

Figure 12: Schematic of FM characterization of peptides

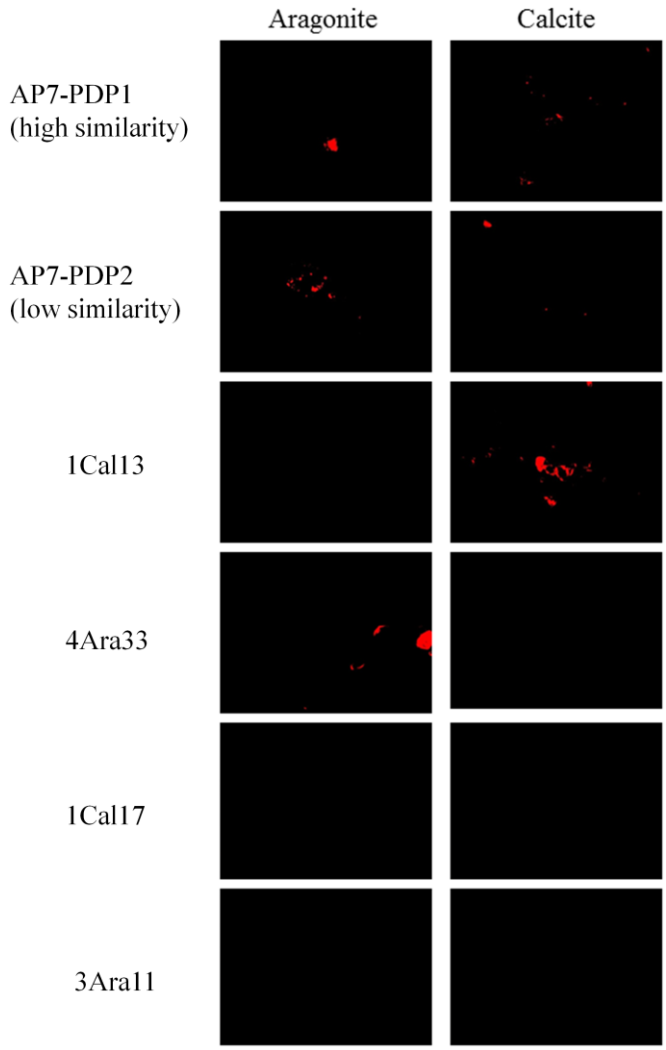

Figure 13: FM images of biotinylated peptide on aragonite and calcite (Images normalized with respect to control). Binding was apparent on both protein derived peptides while 1Cal13 and 4Ara33 were specific to their polymorph.

The threshold calculations were adjusted with respect to how much substrate was shown in the sample field. For instance 100% coverage would be maximum coverage of all the crystals shown in the bright-field image rather than complete coverage of the whole image. Figure 14 shows the threshold measurements of the four peptides tested. From the graph it is clear that even though

AraBP2 is the low similarity binder it in fact binds better to aragonite than its high similarity counterpart. Also both protein derived peptides show binding to calcite though much less than 1Cal13 which shows threshold coverage of about triple theirs. Along with this it appears that two of the peptides do not have any binding to $CaCO_3$ after being removed from the cells. This may be due to the peptide interacting with the biotin and reducing its binding ability to the Qdots. Also the peptide may be interacting with itself and not the substrate which would not happen when it is attached to the cell.

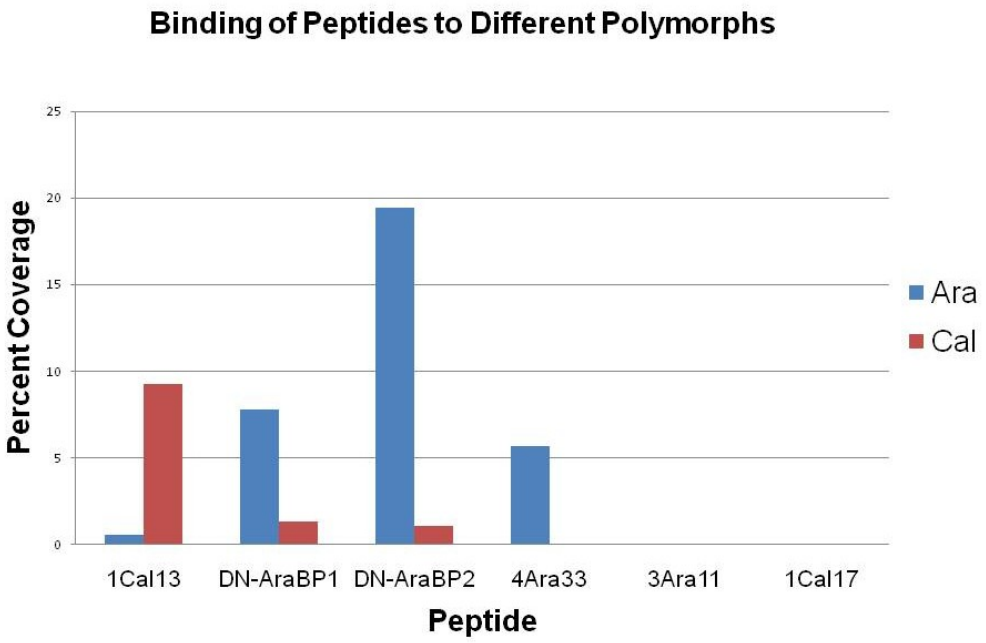

Figure 14: Percent coverage calculations for the peptides. (Threshold measurements were done using Metamorph software).

3.4. Optimization of Procedures

3.4.1. Optimization of Calcite formation

Calcite formation was optimized to only produce this polymorph insure that they have all have similar morphologies. Three different approaches were found in the literature that would make calcite consistently. For some of the approaches the researcher mixed $CaCl_2$ with Na_2CO_3 or $NaHCO_3$ at different concentrations and another used NH_4CO_3 in a dessicator with the $CaCl_2$. After trying all of the methods listed above only the NH_4CO_3 consistently produced only calcite, while the others would sometimes produce a mixture of calcite and vaterite. Along with this the dessicator approach allowed the peptide the longest time to interact with the solution before

crystals formed. This approach is also a slightly better mimic of nature in the fact that there is slow addition of carbon dioxide rather than it being instantaneous, which is probably why many researchers prefer this method.

Further optimization was done on the dessicator method since many researchers have slight modifications that can often times change the results of peptide addition considerably. The two main optimizations for the control were in altering the amount of solution and taking samples from the bottom, middle and top of the solution for SEM and XRD. Unfortunately, when reducing the amount of solution below 10ml there was not enough crystals in the solution to be able to get an accurate XRD reading. TEM was also tried for polymorph identification in the smaller solutions, but the crystals were too big to be able to get a diffraction pattern from them. The crystals would also often break the TEM grid which is why this method is not used for characterization. For this reason a 10ml solution was used in all of the peptide mineralization experiments. As for taking SEM and XRD samples from different locations in the petri dish the bottom of the solution had highest concentration of crystals and so would give a better signal in the XRD compared to the middle and top of the petri dish. Also for the SEM images there was very little difference between layers in terms of morphology unless it was at the top of the solution at which point there was very little $CaCO_3$ crystals and a lot of salts.

3.4.2. Optimization of Aragonite formation

Several optimization steps were needed in order to create aragonite consistently without raising the temperature above a level that would be harmful to the peptide. The procedures were modified in order to create the same level of aragonite every time if a mixture developed. Percentages of the different polymorphs were determined by the equations developed by Kontoyannis et al, where X is the molar fractions of the polymorph aragonite (A), calcite (C), and vaterite (V). [63] The intensities for the peak are represented as I with the peak number and the polymorph symbol.

[2] $$X_A = \frac{1.395 \times I_A^{700}}{I_C^{711} + 1.395 \times I_A^{700} + 9.30 \times I_V^{750}}$$

[3] $$X_C = \frac{X_A \times I_C^{711}}{1.395 \times I_A^{700}}$$

[4] $$X_V = 1.0 - X_A - X_C$$

Several different procedures found in the literature have been used to create aragonite that do not raise the temperature and would not take several weeks to complete. Figure 15 shows the composition of $CaCO_3$ at different temperatures and that you need to go above 100°C in order to get only aragonite formation.[64] An approach developed by Ahn et al was tried that has 0.2 moles of $Ca(OH)_2$ and 0.8 moles of $MgCl_2$ mixed with 10mls water at pH 8.7 and put in a dessicator with $(NH_4)_2CO_3$ overnight to form aragonite.[65] Aragonite was not developed for this approach but instead a mixture of ammonium magnesium chloride hydrate, magnesium chloride hydrate, $Mg(OH)_2$ and calcite was formed instead.

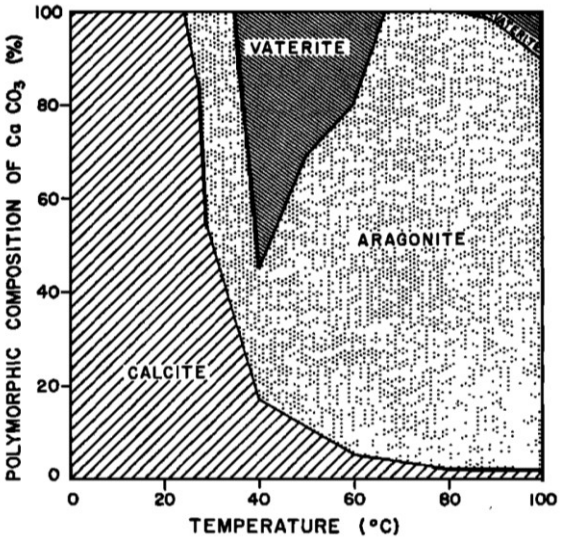

Figure 15: Composition diagram of $CaCO_3$ using the $Ca(HCO_3)$-CO_2-H_2O approach without MgCl.[64]

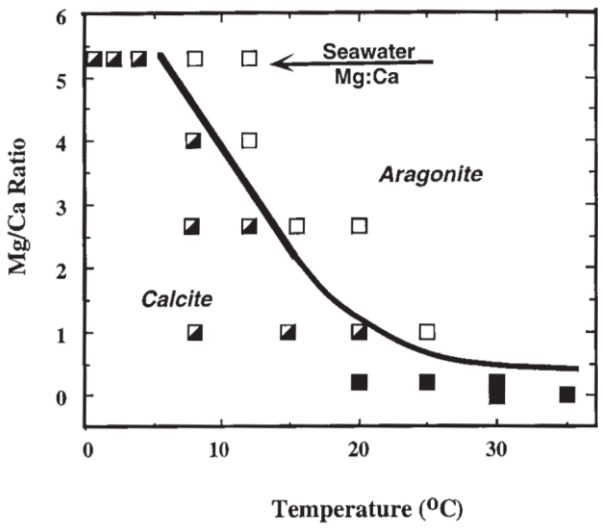

Figure 16: $CaCO_3$ polymorph formed at different ratios of Mg:Ca and temperatures. White squares are aragonite, black is calcite and mix is situations where calcite initially precipitates and then aragonite grows on top of it. [12]

After the Ahn approach failed to produce aragonite, an Mg addition approach was used based on the ratio between the ions. Figure 16 shows which polymorph should develop based on the ratio of Mg to Ca using a slow addition of carbon dioxide.[12] This figure was used to determine the

level of Mg to add to the two different approaches to form aragonite. The first approach was the optimized calcite procedure with a dessicator filled with NH_4CO_3 and then adding Mg to the $CaCl_2$ solution. The second approach was adding Mg to a $CaCl_2$ solution and then adding $NaHCO_3$ to this solution. Both of these approaches yielded aragonite as well as many other materials, but the NH_4CO_3 was more consistent in getting the percentage of aragonite to be around 25% of the mixture and so was used for the peptide addition studies.

3.5. Mineralization with Peptides

3.5.1. Calcite Formation with Peptides

All of the selected peptides and two protein derived peptides were used in gas diffusion experiments in order to compare results with other literature studies. The starting pH values were not changed and range from around pH of 4-7 and the ending pH is around 8-9. All the peptides were tested at a concentration of 0.1mM. Those that showed interesting results were tested at two other concentrations of 0.05mM and 5mM. The higher concentration could not be tested on the XRD since not enough crystals were developed indicating that at high enough concentrations the peptides are inhibiting the formation of crystals. The mineral is then analyzed using SEM for the morphology and XRD to accurately quantify the polymorphs and their concentrations.

SEM analysis

As shown in figure 16 many of the peptides show what appears to be considerable vaterite development in all cases compared to the control which shows only calcite development for the gas diffusion experiments. From Fig 17 (a) and (b) it appears that both 4Ara17 and 1Cal17 do not affect the morphology of the calcite crystals except a slight amount of etching at the 0.1mM concentration. The peptide 3Ara11 on the other hand was very unusual in the fact that it would sometimes create what appeared to be vaterite but it was not consistent in doing so even at the same conditions as seen from Fig 17 (c) and (d) which shows the vaterite when it was developed and the calcite which did not have any morphology change. When 3Ara11 did form vaterite it would sometimes have a very unusual morphology where the vaterite hexagonal platelets appeared to go from stacking normally to randomly stacking in different directions as seen in (c). Adding 0.1mM of 4Ara33 appears to form a mixture of regular spherical vaterite and calcite which appears to have many calcite crystals fused together as seen from Fig 17 (e) and (f). At lower concentrations of peptide the calcite is similar to that of the control and the vaterite looks the same as the slightly higher concentration. The highest concentration of 5mM the vaterite is

covered by a layer of organic, though still seems to maintain its spherical shape though it is hard to tell due to the organic covering. For the 1Cal13 peptide there is no difference from the control at the low concentration of 0.05mM, but at 0.1mM, flower like vaterite begins forming along with very highly etched calcite as seen in Fig 17 (g) and (h). The protein derived peptides both produced what appeared to be a mixture of vaterite and calcite at 0.1mM, though the morphologies of the vaterite differ depending on which peptide was added. As seen in Fig 17 (i), AP7-PDP1, the high similarity protein derived peptide, produced vaterite that appears to be many small vaterite spheres arranged in a ring fashion and stacked on top of each other. The low similarity protein, AP7-PDP2, on the other hand has these vaterite spheres attached to one point localized in the center which is seen in Fig 17 (j). Control solutions that had no peptide added were run during each set of experiments and showed similar results to Fig 17(k). The morphology developed by AP7-PDP2 appears to be unique to this peptide in the fact that no other researchers have yet shown this morphology using peptide, protein or polymer. On the other hand the morphology of the vaterite developed by the 4Ara33 is pretty standard in terms of how it could be developed, but the calcite morphology is also unique to this peptide. The 1Cal13 creates vaterite similar to one of Coelfen's polymers, PEG(45)-b-PGL(27), that was found to also rely heavily on the surface tension of the solution.[66] How these different morphologies could have been developed is explained further in the discussion section. XRD was used to confirm that many of these morphologies are indeed vaterite.

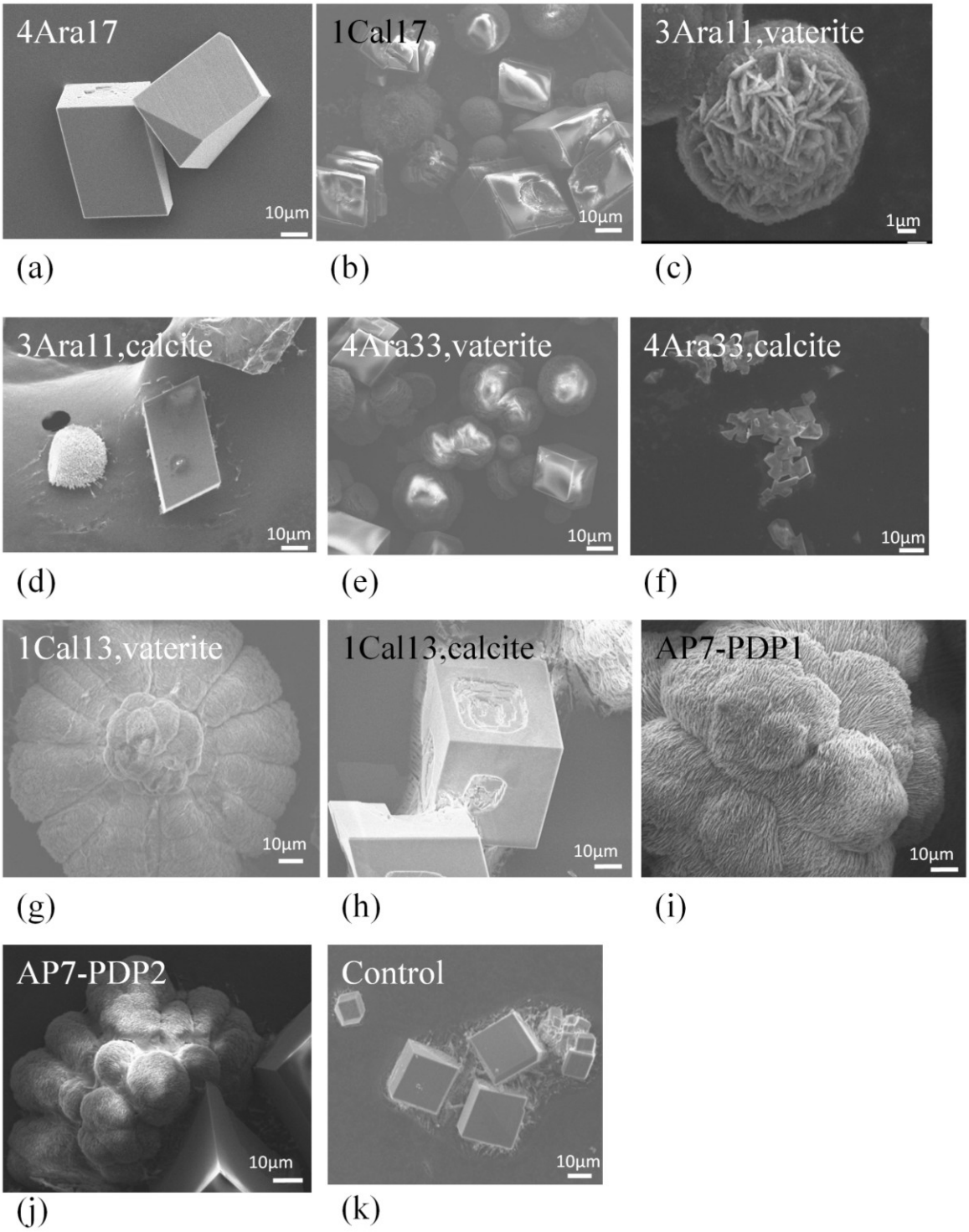

Figure 17: Representative SEM images of $CaCO_3$ developed using the gas diffusion method and with 0.1mM peptides added to the solution. (a) 4Ara17 (b) 1Cal17 (c) 3Ara11, vaterite's morphology (d) 3Ara11, calcite's morphology (e) 4Ara33 vaterite morphology (f) 4Ara33 calcite morphology (g) 1Cal13 vaterite morphology (h) 1Cal13 calcite morphology (i) DN-AraBP1 (j) DN-AraBP2 (k) Control without peptide. All images at 1,000X magnification.

XRD analysis

The XRD was done on at least three different runs for those peptides that produced polymorphs other than calcite to insure reproducibility of the quantification. Figure 18 shows XRDs of each peptide with the different polymorph peaks marked with C for calcite or V for vaterite. There is also a quartz peak marked as a Q on some of the images that is present when the crystals don't cover the entire glass slide. The quartz peaks can also be seen in the control Fig 18 (e) as well as when small amounts of the pure geological calcite is scanned.

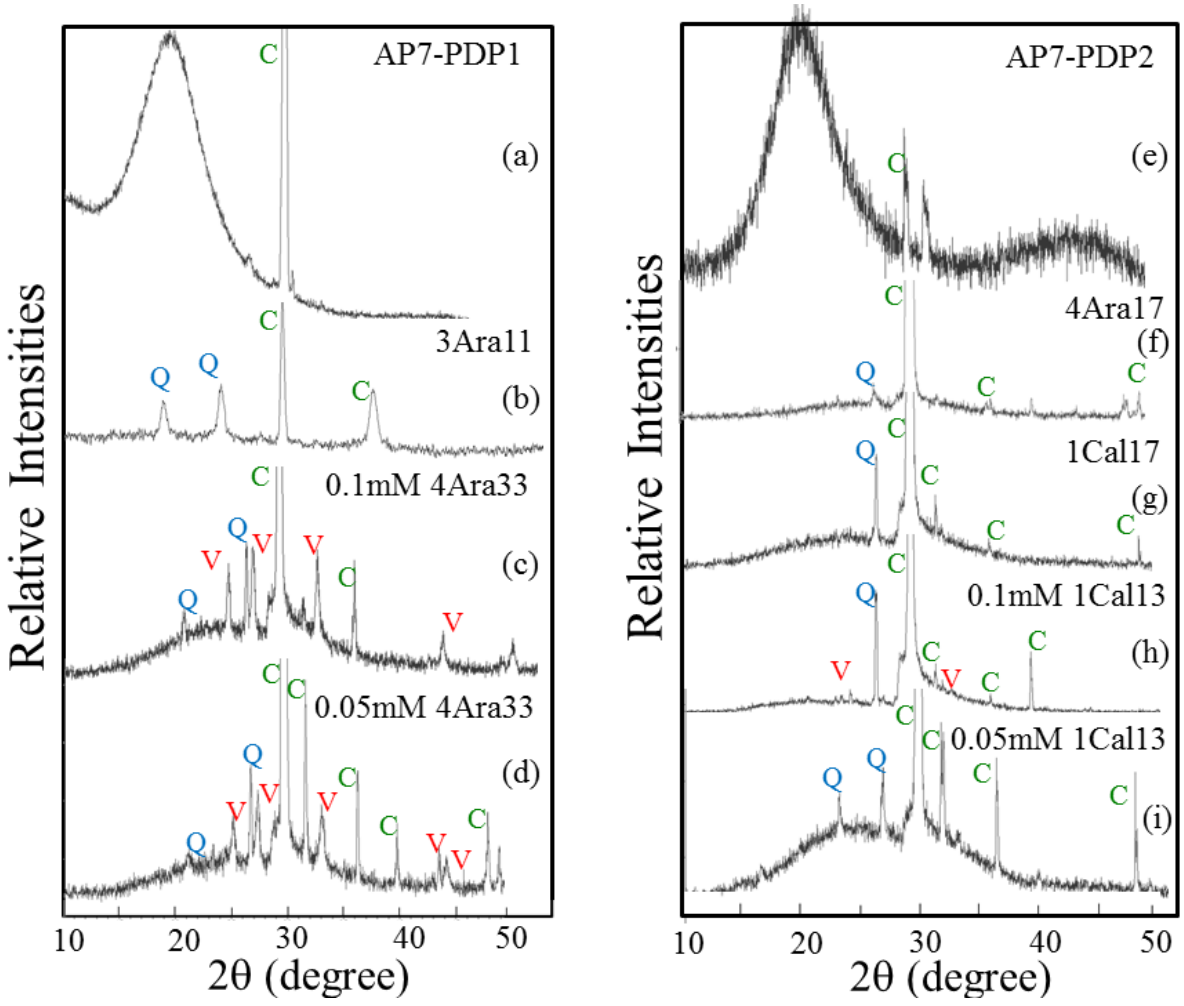

Figure 18: The X-Ray diffraction patterns of crystals created with the incorporation of peptides. (a) 0.1mM DN-AraBP1 (b) 0.1mM 3Ara11 (c) 0.1mM 4Ara33 (d) 0.05mM 4Ara33 (e) No peptide added (f) 0.1mM DN-AraBP2 (g) 0.1mM 4Ara17 (h) 0.1mM 1Cal17 (i) 0.1mM 1Cal13 (j) 0.05mM 1Cal13

For the protein derived peptides there was not enough crystal to produce a clear diffraction pattern reproducibly and would normally show amorphous crystal. On one occasion a single calcite peak was detected for AP7-PDP1 and AP7-PDP2 as seen in Fig 18 (a) and (f) though this

was unable to be reproduced and even in these situations a large amorphous curve was seen. The formation of amorphous crystal in these solutions is unlikely since there is clearly calcite and vaterite crystal morphology in the SEM images of the protein derived peptides as seen in Fig 17. As was clear from the SEM images 4Ara17 and 1Cal17 do not appear to affect the polymorph of $CaCO_3$ since they produce calcite peaks as seen in Fig 18 (g) and (h). Fig 18 (b) shows that 0.1mM of 3Ara11 forms calcite with large quartz peaks since amount of crystal produced was small.

The 4Ara33 and 1Cal13 peptides both produce vaterite at a 0.1mM concentration, which can be seen in Fig 18 (c) and (i). At the lower concentration of 0.05mM the 4Ara33 is still able to produce vaterite, but the 1Cal13 peptide is unable to do so as seen in Fig 18(d) and (j).

Quantification was done using an equation developed by Kontoyannis et al. In their paper they discuss that if one has a mixture of calcite, vaterite and aragonite it is possible to get the ratios of certain peaks and calculate the percentage of each compared to the whole.[63] They also discuss this principle if just two of the components are present. The following equation was used to calculate the percentage of the vaterite to calcite where I_C^{104} stands for intensity of the (104) reflection peak for calcite:

$$\frac{I_C^{104}}{I_V^{110}} = 7.691 \times \frac{X_C}{X_V} \quad [5]$$

This equation can be used for determining the percentage between the calcite and vaterite even if other components are present, unless those materials have similar peaks in the diffraction pattern which could offset the intensity ratio. For this reason the quartz peaks can be ignored since they are not close to the vaterite peak that is used for identification. Figure 19 displays the percentage of vaterite present for two different concentrations of the 4Ara33 peptide and the 1Cal13 peptide. From this graph it is clear that 4Ara33 is able to form more vaterite than 1Cal13, and can form this polymorph at a lower concentration then 1Cal13. The 1Cal13 also has a very large error bar which may be related to the fact that the vaterite morphology from the SEM image appears to

also rely on surface tension, which is very difficult to control.

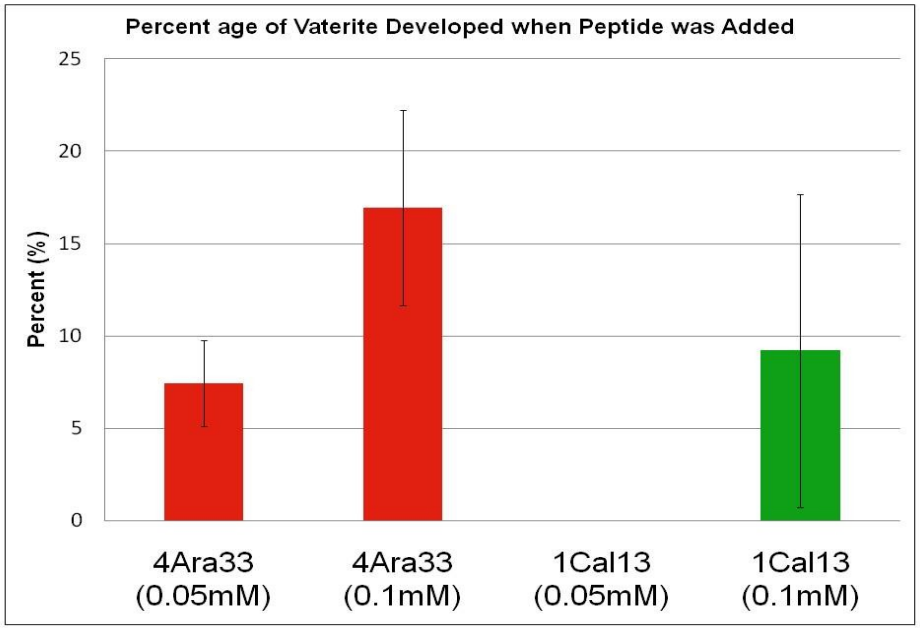

Figure 19: Percentage of vaterite developed for different concentrations of peptide added. Percentages calculated using equation 1.

3.5.2. Aragonite Formation with Peptides

The two peptides that altered the calcium carbonate polymorph, 4Ara33 and 1Cal13 were then used for mineralization in the aragonite forming solution described earlier in the materials and methods section where the . In the control, about 25% of the crystals formed were aragonite as seen from the XRD and SEM in fig 20. Aragonite has a needlelike morphology that all origninate from a single point while the calcite growth is inhibited so that they form flat ovals. When 0.1mM of 4Ara33 was added to the solution a film of unknown crystals were developed since the XRD did not show any peaks which indicates that this layer may be salt and so came off when the slide was rinsed. 1Cal13 also showed flat layering of crystals developing in the SEM and from the XRD they appeared to be calcium nitrate hydrate with a mixture of the three other $CaCO_3$ polymorphs. The calcite nitrate hydrate has a peak very close to the araognite peak that is used for calculations, so the percent aragonite was unable to be determined accurately for comparison with the control.

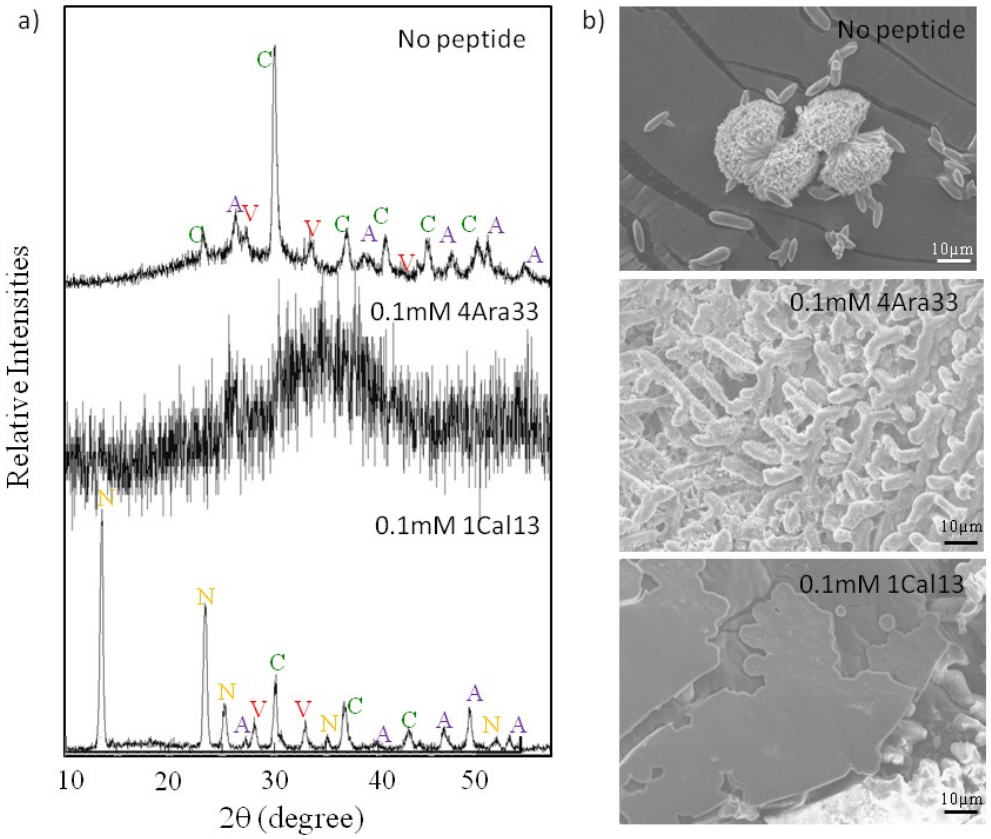

Figure 20: X-ray diffraction and scanning electron microscopy results of peptide addition to aragonite forming solution of 3:1 Mg:Cl ratio solution in a desiccator. (a) XRD and (b) SEM of with no peptide added, 0.1mM 4Ara33 and 0.1mM 1Cal13 added to the solution.

Chapter 4: Discussion

4.1. Peptide Selection

A set of five peptides were selected using cell surface display with a counter selection round to further increase the specificity these peptide have to only one polymorph of $CaCO_3$. Previous studies have used phage display to select peptides that bind to calcite or aragonite, but neither set has shown specificity of their peptides to only one polymorph. Along with this almost all of the peptides that have been previously selected from display systems have been positively charged. Whether this peptide selection criteria is from the phage display preferring positively charged sequences for selection is unknown since none of the studies provide entire selection data or very few peptides were sequenced. In this study we used peptides that varied with charge, hydrophobicity and pI and all of them bound strongly to their respective polymorph when displayed on cells.

The distribution of amino acids for the selected peptides shows some overall trends as well as distinct tendencies for each of the polymorphs. Aspartic acid, a negatively charged molecule, had the highest relative abundance in both the aragonite and calcite binders. In the literature aspartic acid chains have been shown to interact with $CaCO_3$ and create unusual helical or layered morphologies in the calcite so having a high abundance in our selection would be expected.[67] Tryptophan, an aromatic molecule, was also found in many of the sequences both strong and weak, which may be due to van der waals forces being involved with binding to the surface. Distribution for the aragonite binders were found to be very similar between the weak and strong binders with only the amino acid asparigine (Asn) being different. Asn is a polar uncharged amino acid that contains an amide group one carbon from the backbone, while in Glutamine (Gln) this group is two carbons away from the backbone. Both sets of aragonite binders have a slight increase in Gln abundance, while there are fewer Asn in the weak binders and the expected abundance for the strong binders. One possible explanation is that the nitrogen group is not seen by the inorganic surface in Asn since it is smaller than the other nitrogen containing amino acids which were all selected for. Aragonite peptides also have a higher number of positively charged side groups than the library suggesting that the surface of the aragonite is negatively charged. Calcite binders on the other hand selected for only Lys that is positively charged while Arg and His were found less often than predicted. Aragonite appears to have a slightly higher charge

density than calcite since its relative abundances for charged amino acids are much higher, which is consistent with it being denser.

4.2. Characterization with Cells

Cells expressing peptides were characterized first on the polymorph they were choosen for and then the strong binders were tested for specificity. In the calcite selection a dramatic jump was seen from the medium to strong binders compared to aragonite which increased steadily from low to high affinity. Also the error bars are much larger for the CalBPs compared to AraBPs. Both of these observations may be due to the larger sampling size for calcite and the fact that it was cleaved instead of polished so its surface may be rougher. Differences in magnification were because two different people were counting the cells; Marketa Hnilova did the aragonite binders characterization while I analyzed the calcite binders. Polished aragonite was used because the saw used for cutting left a very uneven surface unsuitable for getting accurate FM results.

4.3. Similarity Analysis

The similarity analysis of calcite indicated that perhaps the line between strong and medium binders may have been set too high, since many of the medium binders were predicted to be strong based on their sequence. The aragonite binders have a few weak binders that were forecasted to be strong perhaps because of their structure or effect on the cells. All of the proteins that were used to find an aragonite domain were associated with the nacre of mollusk shells and two have been shown to form aragonite in vitro. The AP7 domains were promising mainly because the protein by itself is able to form aragonite without any additives using the dessicator method. The protein derived peptides had a considerable amount of charged amino acids, with the high similarity one being mostly negative amino acids while the low similarity had positive ones. Even though aromatics did not have a high relative abundance in our selection both of the de novo designed peptides contained a few of them, which may be due to the AP7 sequence.

4.4. Characterization of synthesized peptides

Binding affinities changed drastically for some of the peptides once they were synthesized, which can be seen in Fig 14. For instance 3Ara11 and 1Cal17 did not show any binding to either polymorph even though they were very strong binders when expressed on the cell. One explanation for this lack of binding in the peptides is that they need to be cyclic in order to

interact correctly. On the cell these peptides are displayed as a loop on the flagella and perhaps this rigid structure is needed to be able to interact with the surface correctly. Another reason for the difference between the characterizations could be that the cells are interacting with the surface by other means than the flagella, though this is unlikely since the cells would then all be close to the same binding affinity. Biotin, a hydrophilic molecule that attaches to streptavidin-Qdots, may also be interfering with the structure of the peptide and not allowing it to bind. Another possibility is that the biotin is folded into the peptide and not able to see the streptavidin-Qdots.

4.5. Mineralization with peptides

Mineralization was done on all of the peptides in a calcite forming environment and peptides that had the ability to control the polymorph were tried in an aragonite forming environment.

In the calcite forming environment several of the peptides had very unique morphologies compared to those found in the literature. 1Cal17, one of the peptides that were found to not bind to the surface also did not affect the morphology or polymorph of the $CaCO_3$. This indicates that binding affinity for calcite binding sequences may play a role in whether a peptide is able to affect the polymorph of $CaCO_3$. 4Ara17, was unable to be biotinylated so the binding affinity is unknown but it also forms calcite that it is similar to the control.

3Ara11, from the FM results also does not have an affinity to either polymorph, but does appear to form an unusual morphology of vaterite under the SEM while the calcite morphology is unchanged. The vaterite appears to have started forming normally with hexagonal platelets stacking on one another and then the platelets switch directions so that they are stack perpendicular to the original in random orientations with each other after that point. This morphology could be due to the peptide interrupting the growth of the vaterite at a certain point and then directing its organization onto a different pathway. The fact that the peptide does not affect the appearance of the calcite in any way is indicative that it does not bind or interact with this polymorph which is confirmed by the FM results. Perhaps 3Ara11 doesn't bind to either calcite or aragonite, but to vaterite. Unfortunately since vaterite is not stable at standard condition the binding affinity of 3Ara11 to it could not be tested. Another explanation for this unusual platelet growth is perhaps the peptide nucleates vaterite at these odd orientations and then when the vaterite is no longer able to see the peptide it starts growing in the normal orientation of this crystal. Unfortunate, the formation of vaterite for this peptide was unable to be

confirmed in the XRD, though from the SEM it appeared to be at least 10% of this polymorph formed most having this unique morphology.

For the aragonite binding peptide, 4Ara33, the vaterite that formed had the same morphology as those formed in the literature when stabilized by polymers. The polymers that are able to create this polymorph often have disordered structures that optimize the number of binding sites indicating that perhaps this peptide also prefers to be disordered. [48] This vaterite formation was confirmed and quantified by XRD. The calcite formed from this peptide actually appeared to form sheets normally with a few separate crystals being separate from these large agglomerations. A similar morphology of layered calcite can be seen in Gower's work concerning poly(asp) chains, though our aragonite binding peptide only contains one aspartic acid residue it might have a similar mechanism of forming these films.[67] In that study the films were made of hexahydrate form of $CaCO_3$, a hydrated phase that forms a platy habit, which then changes into the more stable calcite while still retaining some aspects of the hydrated form.[67] The aragonite peptide may also utilize this mechanism, but it can't be confirmed since the final crystals are calcite and it is difficult to get a diffraction pattern from the hydrated $CaCO_3$.

For the calcite binding peptide, 1Cal13, the vaterite that was formed at 0.1mM concentrations had a flower like morphology similar to that found by Coelfen.[66] They determined that variations in water tension and hydrophobicity were affecting the vaterite superstructure.[66] The flower like vaterite morphologies were normally only found when there was very high surface tension under hydrophilic conditions which occur with phosphorylation.[66] The XRD confirmed that the crystals with these odd flower morphologies found in the SEM were indeed vaterite. In our case 1Cal13 most likely interacts with the vaterite at the surface of the solution stabilizing it and starting formation of the flat platelets next to each other. After the structure gains enough mass to break the surface tension the vaterite is then allowed to stack into a sphere. The vaterite extensions are flat because our peptide is hydrophilic so the superstructure drops from the surface sooner since nothing is keeping it from interacting with the water except surface tension. Calcite formed when 1Cal13 is added to the solution appears to have slightly etched surfaces. This morphology is most likely due to growth inhibition by the peptide binding to the growing edge.

Both of the de novo designed peptides showed vaterite spheres agglomerating into a larger structure though their organization appears to be slightly different as well as calcite crystals that looked similar to the control. Unfortunately, the XRD did not confirm that these spheres are

vaterite, since the amount of peptide was too low to get accurate readings. For the high similarity aragonite binder, AP7-PDP1-AP7, the spheres appeared to be arranged in rings stacked on one another into a larger sphere. AP7-PDP2-AP7 on the other hand had a superstructure where all of spheres appeared to be originating at a single point and growing out into a sphere from there. Even though these peptides had different similarity to the aragonite binding peptides they both appeared to create vaterite and calcite in the mineralization solution. Comparing the sequences one can see why they both behave similar to the selected aragonite binding peptides. Both sequences have a large number of charged groups both positive and negative spread evenly throughout the sequence. Even though AP7-PDP2-AP7 had a number of aromatic amino acids they did not seem to impede in the binding.

Aragonite mineralization was done with the two peptides, 4Ara33 and 1Cal13, that were able to affect the polymorph of calcium carbonate. The same concentration was used in this experiment as the one that created vaterite in the calcite mineralization. For the aragonite mineralization only 25% aragonite is formed in the original mineralization experiment with a mixture of vaterite and calcite present as well. When the aragonite binder is added to the solution a film is formed that could be made up of salt though this was not confirmed with XRD since either the amount of crystal was too low or it was rinsed off prior to analysis. The calcite binder also created a flat film under SEM though this was confirmed under XRD to be a mixture of calcite nitrate hydrate and the three polymorphs of calicum carbonate. Exact aragonite percentages were not able to be found because no formales have been created for mixtures of $CaCO_3$ polymorphs and calcite nitrate hydrate and since this chemical has peaks similar to aragonite it can not be ignored as with quartz.

Chapter 5: Conclusion

In this study, peptides were selected that bound specifically to different polymorphs of calcium carbonate to observe their effect on the crystal structure and morphology. The selection was done using cell surface display with a unique counter selection at the end to insure that the peptides only bound to one crystal structure. The cells were then sequenced and characterized on their particular polymorph into strong, medium and weak binders using FM. The strong binders were then tested for specificity by observing how many of the cells bound on the polymorph they were not selected for. Some of these peptides were then synthesized and characterized further.

A similarity analysis was performed on both sets of binders to see how the different binders compared to each other. The predicative power of the analysis was higher for the aragonite binders than for the calcite, 82% to 64%, indicating that aragonite strong binders are closer in similarity than the calcite ones. From these results we used the aragonite similarity analysis on several natural aragonite binding proteins to determine domains within them that may be responsible for their binding. The domains found in AP7 were chosen to be synthesized because AP7 has been shown to create aragonite in vitro and these domains were not folded inside the protein so could be involved with surface interaction.

The five peptides that were synthesized from the selection all bound strongly to their respective substrate on the cells, but varied in charge and pI. The binding affinity of the selected and the protein derived peptides for many were not consistent with what was seen with the cells. For instance, two of the peptides that showed very strong binding on the cells bound to neither of the substrates. Also the protein derived peptides bound to both polymorphs, but two of the selected peptides were found to preferentially bind to their selected substrate with little to no binding found on the other.

Calcite mineralization with the peptides produced vaterite for several of the peptides many having unique morphologies under SEM. 3Ara11 produced what appeared to be vaterite that has never been seen in the literature where platelets are stacked perpendicular at the end of the normal spherical superstructure. The XRD was unable to confirm vaterite formation expect for in two cases with the specific aragonite and calcite binders, which indicates that binding affinity may play a role in polymorph control. The vaterite percentage in these mixtures was calculated

and found to be related to peptide concentration for the aragonite binding peptide. The calcite binding peptide was only able to produce vaterite at a high enough concentration while at the lower concentrations tested it just formed calcite that showed signs of growth inhibition.

In the aragonite mineralization experiment 1Cal13 was able to produce calcium nitrate hydrate along with the other polymorphs of calcite carbonate in the solution, with the appearance of flat platelets. 4Ara33 was unable to produce enough crystals to be analyzed in the XRD, but under the SEM it also showed a film like substance forming.

Chapter 6: Future Work

Several directions can be taken to further different aspects of this study. One possibility is to create a method for monitoring the kinetics of formation that would consistently produce calcite when no peptide is added. Currently most of the kinetics approaches produce vaterite in addition to calcite. When doing Ca assay's on crystals in the desiccators the results were unable to be repeated and so were not included in this report. Another kinetics approach that was tried was observing the pH change, but it was difficult to get a stable reading in the beginning when the desiccator was used with our pH meter.

Another possible direction is to focus more on creating protein derived peptides and comparing their binding to the natural protein at the same conditions. If similar morphologies develop then it could be indicative that these domains are responsible for the proteins interaction with the surface and can be further investigated. Finding the binding domains of the peptides would be useful in being able to being able to study aspects of the full length peptide without needing to synthesis it entirely.

Beta-Chitin could also be used in combination with the selected and protein derived peptides to see if this interaction could form aragonite in the calcite approach. These studies would hopefully show results similar to John Evans approach that he uses for the N16 protein, where he is able to create aragonite when protein is added.[68] If that is the case then the peptides maybe stabilizing aragonite in a similar fashion to the natural proteins.

Growth studies on calcite crystals could be done to observe how the binding strength affects the growth of a substrate in solution. Liquid mode atomic force microscopy (AFM) could be used to test whether the peptides are influencing the growth of certain crystal strucutres when in a Ca^{+} rich environment. These studies would be able to show whether the 1Cal13 is actually etching the surface of the calcite crystal or inhibiting the growth of certain planes. Also this study would tell us whether the peptides could change the polymorph on the surface or if it is only affecting the ions in solution.

Structure analysis of the peptides in a solution that contains ions of Ca^{+} and Mg^{+} could be done to see how the peptide's structure is affected when presented with these elements. Along with this we could model how their structure changes when presented with different polymorph surfaces. These structures could then help us make mutations to test whether the mechanism of binding is correct. Mutations could then be done to see how important certain amino acids are to the function of the peptide. One possible mutation would be removing the charged groups from the sequences and seeing if the peptide would still bind or change the polymorph of the crystal.

Chapter 7: Bibliography

(1) Meldrum, F. C., Calcium carbonate in biomineralisation and biomimetic chemistry. *International Materials Reviews* **2003,** 48, (3), 187-224.

(2) Mann, S., *Biomimetic Materials Chemistry*. ed.; John Wiley & Sons: 1995.

(3) Sarikaya, M.; Aksay, I. A., *Biomimetics: design and processing of materials*. ed.; AIP Press: 1995.

(4) Sarikaya, M., Biomimetics: Materials fabrication through biology. *Proceedings of the National Academy of Sciences of the United States of America* **1999,** 96, (25), 14183-14185.

(5) Lippmann, F., *Sedimentary carbonate minerals*. ed.; Springer-Verlag: Berlin, New York,, 1973; p vi, 228 p.

(6) Reeder, R. J.; Mineralogical Society of America., *Carbonates : mineralogy and chemistry*. ed.; Mineralogical Society of America: Washington, D.C., 1983; p xii, 394 p.

(7) Kulik, D. A.; Vinograd, V. L.; Paulsen, N.; Winkler, B., (Ca,Sr)CO3 aqueous-solid solution systems: From atomistic simulations to thermodynamic modelling. *Physics and Chemistry of the Earth* **2010,** 35, (6-8), 217-232.

(8) Ji, B. H.; Gao, H. J., Mechanical properties of nanostructure of biological materials. *Journal of the Mechanics and Physics of Solids* **2004,** 52, (9), 1963-1990.

(9) Mayer, G.; Sarikaya, M., Rigid biological composite materials: Structural examples for biomimetic design. *Experimental Mechanics* **2002,** 42, (4), 395-403.

(10) Mayer, G., Rigid biological systems as models for synthetic composites. *Science* **2005,** 310, (5751), 1144-1147.

(11) Wilbur, K. M.; Bernhardt, A. M., EFFECTS OF AMINO-ACIDS, MAGNESIUM, AND MOLLUSCAN EXTRAPALLIAL FLUID ON CRYSTALLIZATION OF CALCIUM-CARBONATE - INVITRO EXPERIMENTS. *Biological Bulletin* **1984,** 166, (1), 251-259.

(12) Morse, J. W.; Wang, Q. W.; Tsio, M. Y., Influences of temperature and Mg:Ca ratio on CaCO3 precipitates from seawater. *Geology* **1997,** 25, (1), 85-87.

(13) Ries, J. B., Aragonite production in calcite seas: effect of seawater Mg/Ca ratio on the calcification and growth of the calcareous alga Penicillus capitatus. *Paleobiology* **2005,** 31, (3), 445-458.

(14) Cheng, X. G.; Varona, P. L.; Olszta, M. J.; Gower, L. B., Biomimetic synthesis of calcite films by a polymer-induced liquid-precursor (PILP) process 1. Influence and incorporation of magnesium. *Journal of Crystal Growth* **2007,** 307, (2), 395-404.

(15) Jacob, D. E.; Soldati, A. L.; Wirth, R.; Huth, J.; Wehrmeister, U.; Hofmeister, W., Nanostructure, composition and mechanisms of bivalve shell growth. *Geochimica Et Cosmochimica Acta* **2008,** 72, (22), 5401-5415.

(16) Trubitt, M. B. D., The production and exchange of marine shell prestige goods. *Journal of Archaeological Research* **2003,** 11, (3), 243-277.

(17) Cats, A.; Kleibeuker, J. H.; Vandermeer, R.; Kuipers, F.; Sluiter, W. J.; Hardonk, M. J.; Oremus, E.; Mulder, N. H.; Devries, E. G. E., RANDOMIZED, DOUBLE-BLINDED, PLACEBO-CONTROLLED INTERVENTION STUDY WITH SUPPLEMENTAL CALCIUM IN FAMILIES WITH HEREDITARY NONPOLYPOSIS COLORECTAL-CANCER. *Journal of the National Cancer Institute* **1995,** 87, (8), 598-603.

(18) Mortensen, L.; Charles, P., Bioavailability of calcium supplements and the effect of vitamin D: Comparisons between milk, calcium carbonate, and calcium carbonate plus vitamin D. *American Journal of Clinical Nutrition* **1996,** 63, (3), 354-357.
(19) Gigac, J.; Kuna, V.; Schwartz, J., EFFECTS OF FIBERS AND FILLERS ON THE OPTICAL AND MECHANICAL CHARACTERISTICS OF PAPER. *Tappi Journal* **1995,** 78, (2), 162-167.
(20) Belcher, A. M.; Wu, X. H.; Christensen, R. J.; Hansma, P. K.; Stucky, G. D.; Morse, D. E., Control of crystal phase switching and orientation by soluble mollusc-shell proteins. *Nature* **1996,** 381, (6577), 56-58.
(21) Falini, G.; Albeck, S.; Weiner, S.; Addadi, L., Control of aragonite or calcite polymorphism by mollusk shell macromolecules. *Science* **1996,** 271, (5245), 67-69.
(22) Tohse, H.; Saruwatari, K.; Kogure, T.; Nagasawa, H.; Takagi, Y., Control of Polymorphism and Morphology of Calcium Carbonate Crystals by a Matrix Protein Aggregate in Fish Otoliths. *Crystal Growth & Design* **2009,** 9, (11), 4897-4901.
(23) Fu, G.; Valiyaveettil, S.; Wopenka, B.; Morse, D. E., CaCO3 biomineralization: Acidic 8-kDa proteins isolated from aragonitic abalone shell nacre can specifically modify calcite crystal morphology. *Biomacromolecules* **2005,** 6, (3), 1289-1298.
(24) Miyamoto, H.; Miyashita, T.; Okushima, M.; Nakano, S.; Morita, T.; Matsushiro, A., A carbonic anhydrase from the nacreous layer in oyster pearls. *Proceedings of the National Academy of Sciences of the United States of America* **1996,** 93, (18), 9657-9660.
(25) Kim, I. W.; Collino, S.; Morse, D. E.; Evans, J. S., A crystal modulating protein from molluscan nacre that limits the growth of calcite in vitro. *Crystal Growth & Design* **2006,** 6, (5), 1078-1082.
(26) Collino, S.; Kim, I. W.; Evans, J. S., Identification of an "acidic" C-terminal mineral modification sequence from the mollusk shell protein Asprich. *Crystal Growth & Design* **2006,** 6, (4), 839-842.
(27) Kim, I. W.; DiMasi, E.; Evans, J. S., Identification of mineral modulation sequences within the nacre-associated oyster shell protein, n16. *Crystal Growth & Design* **2004,** 4, (6), 1113-1118.
(28) Shen, X. Y.; Belcher, A. M.; Hansma, P. K.; Stucky, G. D.; Morse, D. E., Molecular cloning and characterization of lustrin A, a matrix protein from shell and pearl nacre of Haliotis rufescens. *Journal of Biological Chemistry* **1997,** 272, (51), 32472-32481.
(29) Amos, F. F.; Destine, E.; Ponce, C. B.; Evans, J. S., The N- and C-Terminal Regions of the Pearl-Associated EF Hand Protein, PFMG1, Promote the Formation of the Aragonite Polymorph in Vitro. *Crystal Growth & Design* **2010,** 10, (10), 4211-4216.
(30) Samata, T.; Hayashi, N.; Kono, M.; Hasegawa, K.; Horita, C.; Akera, S., A new matrix protein family related to the nacreous layer formation of Pinctada fucata. *Febs Letters* **1999,** 462, (1-2), 225-229.
(31) Weiss, I. M.; Kaufmann, S.; Mann, K.; Fritz, M., Purification and characterization of perlucin and perlustrin, two new proteins from the shell of the mollusc Haliotis laevigata. *Biochemical and Biophysical Research Communications* **2000,** 267, (1), 17-21.
(32) Amos, F. F.; Ndao, M.; Evans, J. S., Evidence of Mineralization Activity and Supramolecular Assembly by the N-Terminal Sequence of ACCBP, a Biomineralization Protein That Is Homologous to the Acetylcholine Binding Protein Family. *Biomacromolecules* **2009,** 10, (12), 3298-3305.

(33) Michenfelder, M.; Fu, G.; Lawrence, C.; Weaver, J. C.; Wustman, B. A.; Taranto, L.; Evans, J. S.; Morsel, D. E., Characterization of two molluscan crystal-modulating biomineralization proteins and identification of putative mineral binding domains. *Biopolymers* **2003,** 70, (4), 522-533.
(34) Evans, J. S., "Tuning in" to Mollusk Shell Nacre- and Prismatic-Associated Protein Terminal Sequences. Implications for Biomineralization and the Construction of High Performance Inorganic-Organic Composites. *Chemical Reviews* **2008,** 108, (11), 4455-4462.
(35) Suzuki, M.; Murayama, E.; Inoue, H.; Ozaki, N.; Tohse, H.; Kogure, T.; Nagasawa, H., Characterization of Prismalin-14, a novel matrix protein from the prismatic layer of the Japanese pearl oyster (Pinctada fucata). *Biochemical Journal* **2004,** 382, 205-213.
(36) Tsukamoto, D.; Sarashina, I.; Endo, K., Structure and expression of an unusually acidic matrix protein of pearl oyster shells. *Biochemical and Biophysical Research Communications* **2004,** 320, (4), 1175-1180.
(37) Keene, E. C.; Evans, J. S.; Estroff, L. A., Matrix Interactions in Biomineralization: Aragonite Nucleation by an Intrinsically Disordered Nacre Polypeptide, n16N, Associated with a beta-Chitin Substrate. *Crystal Growth & Design* **2010,** 10, (3), 1383-1389.
(38) Norizuki, M.; Samata, T., Distribution and function of the nacrein-related proteins inferred from structural analysis. *Marine Biotechnology* **2008,** 10, (3), 234-241.
(39) Amos, F. F.; Evans, J. S., AP7, a Partially Disordered Pseudo C-RING Protein, Is Capable of Forming Stabilized Aragonite in Vitro. *Biochemistry* **2009,** 48, (6), 1332-1339.
(40) Ndao, M.; Keene, E.; Amos, F. F.; Rewari, G.; Ponce, C. B.; Estroff, L.; Evans, J. S., Intrinsically Disordered Mollusk Shell Prismatic Protein That Modulates Calcium Carbonate Crystal Growth. *Biomacromolecules* **2010,** 11, (10), 2539-2544.
(41) Wustman, B. A.; Weaver, J. C.; Morse, D. E.; Evans, J. S., Characterization of a Ca(II)-, mineral-interactive polyelectrolyte sequence from the adhesive elastomeric biomineralization protein lustrin A. *Langmuir* **2003,** 19, (22), 9373-9381.
(42) Wustman, B. A.; Morse, D. E.; Evans, J. S., Structural characterization of the N-terminal mineral modification domains from the molluscan crystal-modulating biomineralization proteins, AP7 and AP24. *Biopolymers* **2004,** 74, (5), 363-376.
(43) Wustman, B. A.; Weaver, J. C.; Morse, D. E.; Evans, J. S., Structure-function studies of the Lustrin A polyelectrolyte domains, RKSY and D4. *Connective Tissue Research* **2003,** 44, 10-15.
(44) Kim, Y. Y.; Douglas, E. P.; Gower, L. B., Patterning inorganic (CaCO3) thin films via a polymer-induced liquid-precursor process. *Langmuir* **2007,** 23, (9), 4862-4870.
(45) Gower, L. B.; Odom, D. J., Deposition of calcium carbonate films by a polymer-induced liquid-precursor (PILP) process. *Journal of Crystal Growth* **2000,** 210, (4), 719-734.
(46) Dai, L. J.; Cheng, X. G.; Gower, L. B., Transition Bars during Transformation of an Amorphous Calcium Carbonate Precursor. *Chemistry of Materials* **2008,** 20, (22), 6917-6928.
(47) Gong, H. F.; Pluntke, M.; Marti, O.; Walther, P.; Gower, L.; Colfen, H.; Volkmer, D., Multilayered CaCO3/block-copolymer materials via amorphous precursor to crystal transformation. *Colloids and Surfaces a-Physicochemical and Engineering Aspects* **2010,** 354, (1-3), 279-283.

(48) Kasparova, P.; Antonietti, M.; Colfen, H., Double hydrophilic block copolymers with switchable secondary structure as additives for crystallization control. *Colloids and Surfaces a-Physicochemical and Engineering Aspects* **2004,** 250, (1-3), 153-162.
(49) Xu, A. W.; Dong, W. F.; Antonietti, M.; Colfen, H., Polymorph switching of calcium carbonate crystals by polymer-controlled crystallization. *Advanced Functional Materials* **2008,** 18, (8), 1307-1313.
(50) Song, R. Q.; Colfen, H.; Xu, A. W.; Hartmann, J.; Antonietti, M., Polyelectrolyte-Directed Nanoparticle Aggregation: Systematic Morphogenesis of Calcium Carbonate by Nonclassical Crystallization. *Acs Nano* **2009,** 3, (7), 1966-1978.
(51) Nassif, N.; Gehrke, N.; Pinna, N.; Shirshova, N.; Tauer, K.; Antonietti, M.; Colfen, H., Synthesis of stable aragonite superstructures by a biomimetic crystallization pathway. *Angewandte Chemie-International Edition* **2005,** 44, (37), 6004-6009.
(52) Xu, A. W.; Antonietti, M.; Yu, S. H.; Colfen, H., Polymer-mediated mineralization and self-similar mesoscale-organized calcium carbonate with unusual superstructures. *Advanced Materials* **2008,** 20, (7), 1333-+.
(53) Kim, I. W.; Morse, D. E.; Evans, J. S., Molecular characterization of the 30-AA N-terminal mineral interaction domain of the biomineralization protein AP7. *Langmuir* **2004,** 20, (26), 11664-11673.
(54) Metzler, R. A.; Kim, I. W.; Delak, K.; Evans, J. S.; Zhou, D.; Beniash, E.; Wilt, F.; Abrecht, M.; Chiou, J. W.; Guo, J. H.; Coppersmith, S. N.; Gilbert, P., Probing the organic-mineral interface at the molecular level in model biominerals. *Langmuir* **2008,** 24, (6), 2680-2687.
(55) DeOliveira, D. B.; Laursen, R. A., Control of calcite crystal morphology by a peptide designed to bind to a specific surface. *Journal of the American Chemical Society* **1997,** 119, (44), 10627-10631.
(56) Masica, D. L.; Schrier, S. B.; Specht, E. A.; Gray, J. J., De Novo Design of Peptide-Calcite Biomineralization Systems. *Journal of the American Chemical Society* **2010,** 132, (35), 12252-12262.
(57) Gaskin, D. J. H.; Starck, K.; Vulfson, E. N., Identification of inorganic crystal-specific sequences using phage display combinatorial library of short peptides: A feasibility study. *Biotechnology Letters* **2000,** 22, (15), 1211-1216.
(58) Li, C. M.; Botsaris, G. D.; Kaplan, D. L., Selective in vitro effect of peptides on calcium carbonate crystallization. *Crystal Growth & Design* **2002,** 2, (5), 387-393.
(59) Gebauer, D.; Verch, A.; Borner, H. G.; Colfen, H., Influence of Selected Artificial Peptides on Calcium Carbonate Precipitation - A Quantitative Study. *Crystal Growth & Design* **2009,** 9, (5), 2398-2403.
(60) Hnilova, M.; Oren, E. E.; Seker, U. O. S.; Wilson, B. R.; Collino, S.; Evans, J. S.; Tamerler, C.; Sarikaya, M., Effect of Molecular Conformations on the Adsorption Behavior of Gold-Binding Peptides. *Langmuir* **2008,** 24, (21), 12440-12445.
(61) Oren, E. E.; Tamerler, C.; Sahin, D.; Hnilova, M.; Seker, U. O. S.; Sarikaya, M.; Samudrala, R., A novel knowledge-based approach to design inorganic-binding peptides. *Bioinformatics* **2007,** 23, (21), 2816-2822.
(62) Page, M. G.; Colfen, H., Improved control of CaCO3 precipitation by direct carbon dioxide diffusion: Application in mesocrystal assembly. *Crystal Growth & Design* **2006,** 6, (8), 1915-1920.

(63) Kontoyannis, C. G.; Vagenas, N. V., Calcium carbonate phase analysis using XRD and FT-Raman spectroscopy. *Analyst* **2000,** 125, (2), 251-255.
(64) Kitano, Y.; Hood, D. W.; Park, K., PURE ARAGONITE SYNTHESIS. *Journal of Geophysical Research* **1962,** 67, (12), 4873-&.
(65) Ahn, J. W.; Choi, K. S.; Yoon, S. H.; Kim, H., Synthesis of aragonite by the carbonation process. *Journal of the American Ceramic Society* **2004,** 87, (2), 286-288.
(66) Rudloff, J.; Colfen, H., Superstructures of temporarily stabilized nanocrystalline CaCO3 particles: Morphological control via water surface tension variation. *Langmuir* **2004,** 20, (3), 991-996.
(67) Gower, L. A.; Tirrell, D. A., Calcium carbonate films and helices grown in solutions of poly(aspartate). *Journal of Crystal Growth* **1998,** 191, (1-2), 153-160.
(68) Keene, E. C.; Evans, J. S.; Estroff, L. A., Silk Fibroin Hydrogels Coupled with the n16N-beta-Chitin Complex An in Vitro Organic Matrix for Controlling Calcium Carbonate Mineralization. *Crystal Growth & Design* **2010,** 10, (12), 5169-5175.